
USF Tampa Graduate Theses and Dissertations

USF Graduate Theses and Dissertations

3-23-2015

An Experimental Study on Passive Dynamic Walking

Philip Andrew Hatzitheodorou
University of South Florida, philip10@mail.usf.edu

Follow this and additional works at: <https://digitalcommons.usf.edu/etd>

 Part of the Biomechanical Engineering Commons

Scholar Commons Citation

Hatzitheodorou, Philip Andrew, "An Experimental Study on Passive Dynamic Walking" (2015). *USF Tampa Graduate Theses and Dissertations*.
<https://digitalcommons.usf.edu/etd/5498>

This Thesis is brought to you for free and open access by the USF Graduate Theses and Dissertations at Digital Commons @ University of South Florida. It has been accepted for inclusion in USF Tampa Graduate Theses and Dissertations by an authorized administrator of Digital Commons @ University of South Florida. For more information, please contact digitalcommons@usf.edu.

An Experimental Study on Passive Dynamic Walking

by

Philip Hatzitheodorou

A thesis submitted in partial fulfillment
of the requirements for the degree of
Master of Science in Mechanical Engineering
Department of Mechanical Engineering
College of Engineering
University of South Florida

Major Professor: Kyle B. Reed, Ph.D.
Stephanie Carey, Ph.D.
Luther Palmer, Ph.D.

Date of Approval:
March 23, 2015

Keywords: Gait, 3D Printing, Passive Dynamic Walker, Rehabilitation, Rapid Prototyping

Copyright © 2015, Philip Hatzitheodorou

Acknowledgments

I would not have been able to complete this project without the support of numerous people along with the support of my family and friends. First, I would like to thank Dr. Kyle B. Reed for giving me the opportunity to work in his lab. I gained invaluable knowledge of engineering and professionalism. The REED Lab is a place that allows freedom of work and thought.

In particular, I would like to thank Dr. Ismet Handzic for his aid in simulation and analysis. It is because of the tools he developed that I was able to complete my work. Katie Hart, thank you for your help in the final stages of my thesis; I hope you gained valuable knowledge as an undergraduate assistant. Jeremy Reedy, although you changed labs, working with you was a pleasure and you expanded my fluency in machining and the manufacturing process.

I thank the rest of my lab mates and co-workers whom I had the privilege of working with. You all provided valuable input for my work as well as challenged and encouraged me. I am fortunate to have you all in my life.

Finally, I would like to thank Dr. Christine Wu who gave me the computer-aided design drawings for Dexter III. Although we have never met nor spoke on the phone, you were willing to support a graduate student 2,000 miles away.

Table of Contents

List of Tables	iii
List of Figures	iv
Abstract	vii
Chapter 1: Introduction	1
Chapter 2: Background	5
2.1 Previous Walkers	5
2.2 PDW Consistency	15
2.3 Model Evolution	16
2.4 3D Printing.....	17
Chapter 3: LUIGI.....	19
3.1 Body Construction	19
3.2 Other Components	23
Chapter 4: Simulation Data.....	24
4.1 Mass Moment of Inertia.....	24
4.2 Damping.....	24
4.3 Foot Shape	27
4.4 Testing Parameters.....	28
Chapter 5: Results	30
5.1 Prior to Simulation.....	30
5.2 Simulation with No Weight	31
5.3 Symmetric (0% - 2%)	33
5.4 Asymmetric Simulation (40% or More)	34
5.5 Asymmetric Physical Results	36
5.6 LUIGI Consistency	36
5.7 Additional Video Analysis.....	36
Chapter 6: Discussion/Conclusions	41
6.1 Issues.....	44
6.2 Recommendations.....	45
List of References	46

Appendices.....	51
Appendix A: 3D Printing	52
Appendix B: Damping	56
Appendix C: Beginning of the Build	62
Appendix D: Trial Figures	63

List of Tables

Table 2.1	Advantages and disadvantages of 3D printing	18
Table 4.1	Experimentally found damping values with data from the CAREN system	27
Table 5.1	Steady state gait with no weight added simulation results from MATLAB for LUIGI	32
Table 5.2	Trial system's asymmetric gait simulation results as well as how much mass to add and where to achieve stated asymmetry.....	35
Table 5.3	Asymmetric gait results for LUIGI	36

List of Figures

Figure 1.1	Gait cycle for a kneed PDW that is composed of a 3-link phase and a 2-link phase	1
Figure 1.2	Humanoid robots.....	3
Figure 2.1	Rimless wheel and synthetic wheel models pioneered by McGeer	6
Figure 2.2	McGeer prototype and Cornell version with knees	7
Figure 2.3	Garcia et al. point foot model that assumes $M \gg m$	7
Figure 2.4	Coleman and Ruina tinker toy	8
Figure 2.5	Wu and Sabet tinker toy	9
Figure 2.6	Honeycutt tinker toy and angle finder	9
Figure 2.7	Toddler robot before and after actuation by Tedrake et al.....	10
Figure 2.8	Version of McGeer's PDW without feet and Museon.....	10
Figure 2.9	Two legged two kneed PDW with arms	11
Figure 2.10	Trifonov and Hashimoto PDW	12
Figure 2.11	Chen PDW	12
Figure 2.12	Honeycutt PDW.....	13
Figure 2.13	Nagoya PDW	14
Figure 2.14	Dexter III	14
Figure 2.15	HM2L	15
Figure 2.16	PDW evolution.....	16

Figure 3.1	LUIGI, based on Dexter III	20
Figure 3.2	PDW thigh comparison	21
Figure 3.3	PDW shank comparison	21
Figure 3.4	Foot, foot bracket and shin of LUIGI made with ABS.....	22
Figure 4.1	Hip damping setup on the CAREN system.....	25
Figure 4.2	Knee damping setup on the CAREN system	25
Figure 4.3	CAD rendering of foot with circle to show the constant radius	28
Figure 4.4	Total length of the upper inner thigh.....	29
Figure 4.5	Example of the attachment of weights on LUIGI	29
Figure 5.1	Launcher setup to remove human variability	31
Figure 5.2	Breakdown of the 9 mass kneed walker model.....	32
Figure 5.3	All 0% - 2% asymmetric systems from the simulation	34
Figure 5.4	All 40% or more asymmetric systems from the simulation with trial systems highlighted.....	35
Figure 5.5	Trial 1 angular position, angular velocity, and angular acceleration for the shin and thigh	37
Figure 5.6	Trial 2 angular position, angular velocity, and angular acceleration for the shin and thigh	38
Figure 5.7	Trial 3 angular position, angular velocity, and angular acceleration for the shin and thigh	39
Figure 5.8	Trial 4 angular position, angular velocity, and angular acceleration for the shin and thigh	40
Figure A.1	ABS material data sheet	52
Figure A.2	PLA material data sheet	53
Figure A.3	MakerBot Replicator 2X	54

Figure A.4	MakerBot Replicator Z18	55
Figure B.1	Single hip bearing damping graph	56
Figure B.2	Double hip bearing damping graph	57
Figure B.3	Single hip bearing with lubricant	58
Figure B.4	Double hip bearings with lubricant	59
Figure B.5	Steel knee bearing	60
Figure B.6	Acetal knee bearing.....	61
Figure C.1	LUIGI first assembly	62
Figure D.1	Trial 1	63
Figure D.2	Trial 2	64
Figure D.3	Trial 3	65
Figure D.4	Trial 4	66

Abstract

In this study, a previously designed passive dynamic walker (PDW) is built out of aluminum and plastic. The aim of the study was to produce an asymmetrical PDW and to compare the results to a computer simulation to validate the mathematical model. It also aimed at identifying the limitations of using additive manufacturing to create components for a PDW as well as gain insights on asymmetric systems.

Beginning with a five mass kneed model, parameters were varied to produce up to a nine mass kneed model solution. The nine mass model allows more variability in added mass locations and separates the zeroth, first, and second moments of inertia. To validate asymmetric gait, step length and step time of the prototype were compared to the simulation. The walker, unable to produce a steady gait, failed to match the asymmetric simulation. More than four times the amount of symmetric data was found compared to asymmetric data. Successful runs of symmetric gaits were approximately double than for asymmetric gaits. The reason for unequal successes is thought to be due to greater instability of asymmetric systems. This instability is thought to be due to inertia from a constant state of changing motion. 3D printing proved useful in simplifying components and reducing waste but the polymers used did not have enough strength when mass was added to the system. Joining differing materials on the legs was difficult to keep in place. A smaller more robust design could solve these problems.

This study focused on understanding physically asymmetric PDWs. These simple robots separate the neurological and mechanical controls of walking and are advantageous for studying physical parameters of human gait. Once a reliable asymmetric walker is built, further research could alter the foot shape or knee location to reverse the process, thus having a PDW walk symmetric. Once a walker is successfully reverted from walking asymmetrical to symmetrical,

these parameters could be then applied to human subjects. An example of this would be for prosthetic foot design.

Chapter 1: Introduction

A passive dynamic walker (PDW) is a simple robot that exhibits a stable gait down a slope while only utilizing potential energy due to gravity. PDWs are an attractive source for research because they have a human-like natural gait that is energy efficient. Advancement of PDWs has steadily progressed from an initial focus on robotic gait to the inclusion of their application in rehabilitation [15]. These simple robots are able to exhibit a stable gait pattern while overcoming energy losses from knee lock (knee strike), as well as heel strike inelastic collision events. The heel strikes account for the majority of kinetic energy lost by the system [38]. These (kneed) walkers have two different phases, which repeat throughout its gait cycle. There is the two-link phase, which begins when a knee strike occurs on the swing leg, and the three-link phase, which occurs at the end of the foot rolling and the toe lifts off.

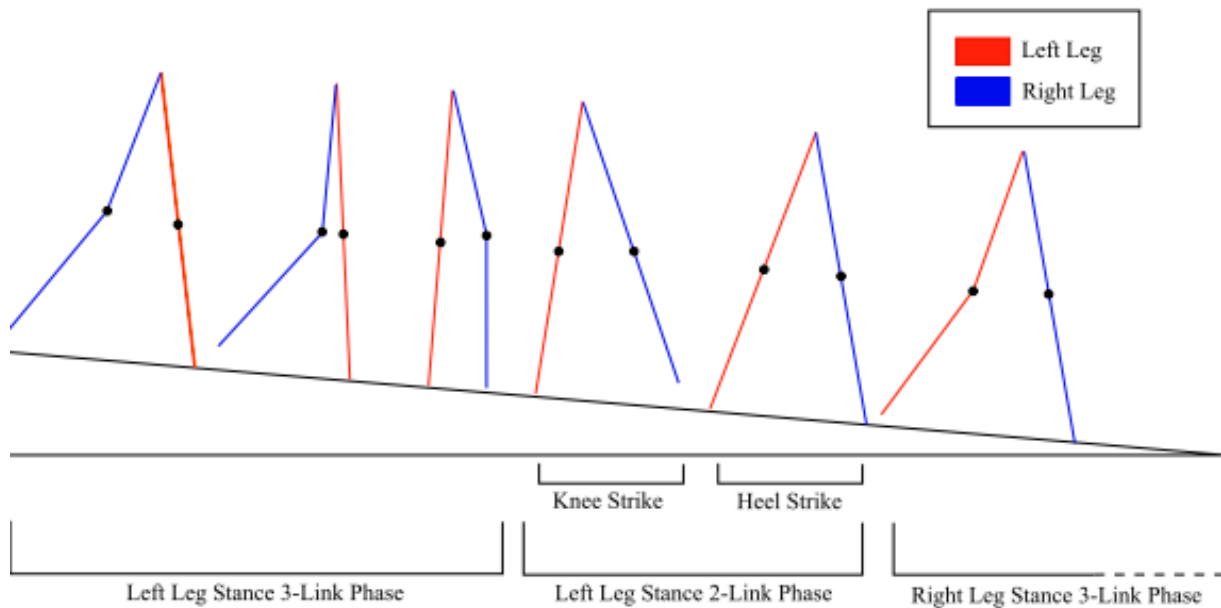


Figure 1.1: Gait cycle for a kneed PDW that is composed of a 3-link phase and a 2-link phase

Ideally, these multi-link pendulum systems exhibit a steady and stable gait when walking, and they have demonstrated their ability to recreate gait that is dynamically similar to humans. Since this is a completely mechanical system, it separates the mechanical and neurological controls of walking, which proves to be advantageous when studying physical parameters of human gait. PDW models are used due to their gait being similar to that of a human [32].

Alternatively, humanoid robots (see Figure 1.2) follow either a quasi-static pattern and/or require controllers to model feedback. Robots such as Toyota's ASIMO [40] and Aldebaran Robotic's NAO [2] are able to simulate slow walking, while Virginia Tech's (in conjunction with the Office of Naval Research) SAFFiR [46] is able to navigate over an uneven floor. Boston Dynamic's Atlas [34] is able to withstand moderate shocks during gait and is able to navigate obstacles. There is also Sandia's second robot, WANDERER [26] but its capabilities will not be showcased until an exposition to be held in conjunction with the DARPA Robotics Challenge Finals in June 2015.

Symmetric gait has been the focus of PDWs as well as humanoid robots. This research aimed to validate models that mathematically demonstrated the possibility of an asymmetric passive dynamic walker and to test the usage of mixed materials when constructing a PDW.

The impact of this research is aim at benefiting rehabilitation. Through previous research, it was shown that training on a split-belt treadmill individuals with an unstable gait are able to regain symmetric gait temporarily [36] [5]. Split-treadmills allow each leg to move at different speeds thus enabling independent control of each. This method creates a symmetric gait, that diminishes over time [37]. A PDW that simulates asymmetric human gait could be used to realize methods for individuals with asymmetric gait to gain symmetric gait in a permanent manner unlike through the use of split-belt treadmills. However, not all asymmetric gait patters are perceived as abnormal. Handzic and Reed [17] used a PDW model to produce walking patterns that showed a degree of abnormality in gait. Step length and step time asymmetries less than 5% were observed as unimpaired and normal. Handzic and Reed [16] validated a previous version of the model used in this experimental study to obtain the simulation results. This was demonstrated by comparing

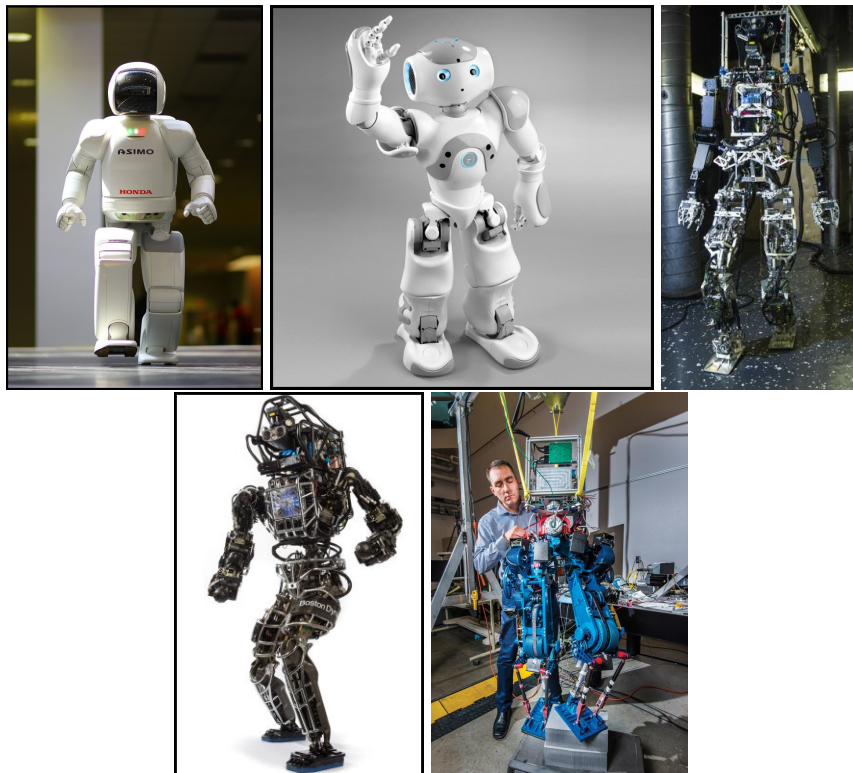


Figure 1.2: Humanoid robots. (Left-Right) Toyota ASIMO, Aldebaran Robotics's NAO, Virginia Tech's SAFFiR, Boston Dynamics Atlas and Sandia's WANDERER. (All images in public domain)

the model to recorded walking data under normal conditions. That PDW model was able to approximate step length, reaction forces, and gait cycle time without joint stiffness and joint damping.

An asymmetric walker has the potential to further develop an understanding of individuals with asymmetric walking patterns and advance solutions for these individual to obtain a natural gait. The walker that is used in this study is LUIGI (Light Unactuated Imitator for Gait Insights), and is based off the University of Manitoba's Dexter III. LUIGI has 3D printed lower sections and is used to verify an asymmetric walking model to help pave the way for future developments for the use of PDWs for rehabilitation purposes.

Chapter 2: Background

Before the term, “Passive Dynamic Walking” was introduced, a few notable researchers hinted toward passive dynamic motion playing a possible role in human walking. Wisse and Linde [47] cite Weber and Weber [45] in 1836 for hypothesizing the similarity of human leg swings to that of a pendulum suspended from a body. In 1958, Ralston [35] discovered that the existence of optimal walking velocity for humans is minimal, which Wisse and Linde [47] noted ”indicates the use of the natural frequencies of the mechanical system”. Mochon and McMahon [33] arrived at the same conclusion as Weber and Weber in 1980 after comparing the swing leg motion to a passive double pendulum.

2.1 Previous Walkers

The actual beginnings of passive dynamic walkers occurred in the late 1980s with the research of McGeer, who is the trailblazer on PDWs [30] [32] [31] [29]. He pioneered the two-dimensional PDW concept by analyzing a rimless wheel rolling down a slope [32], which was first studied by Margaria [27]. During each step, the rimless wheel gains some energy from gravity and loses it at the impact with the ground. With a system in a steady limit cycle there is a balance between energy gained and energy loss. McGeer also contributed to the conception of the synthetic wheel that has a pin joint at the hub, removes all but two spokes, and cuts the rim between the two spokes (see Figure 2.1). Like a passive pendulum the swing leg swings forward, and at the same time the stance leg rolls forward at a constant speed. Initial conditions vary depending on the speed so that the step ends precisely how it began.

Following the inception of the models, McGeer simulated and built a straight-legged passive walker that attained 2D dynamics due to double leg pairs; the outer legs functioned as one

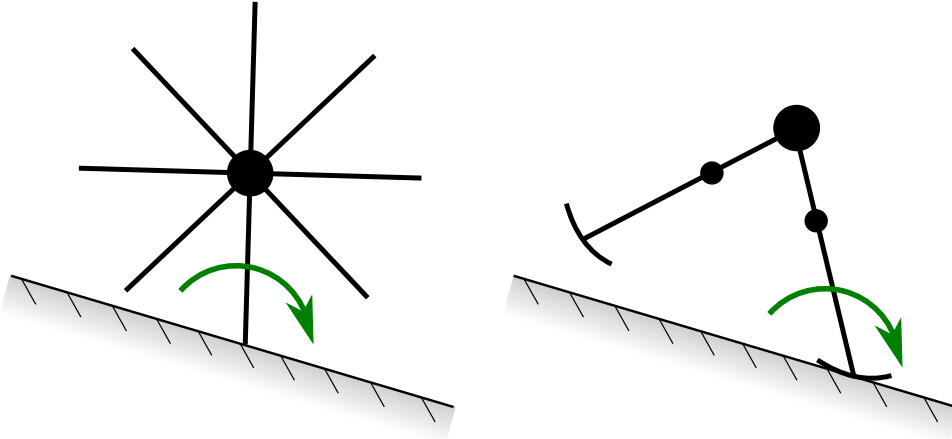


Figure 2.1: Rimless wheel and synthetic wheel models pioneered by McGeer

leg while the inner leg functioned as the second. The walker was not completely passive as it had motors that folded the feet sideways during the swing phase to prevent toe-stubbing. This straight-legged passive dynamic prototype created by McGeer had a leg length of 50 centimeters, weighed 3.5 kilograms, and had a foot radius 1/3 of said leg length, which is said to be a human-like value [18].

In 1998 at Cornell University, Garcia [11] made a version of McGeer's passive dynamic walker with knees and Garcia et al. [10] developed the point foot model (see Figure 2.3). This model is simpler than the synthetic wheel as there is no rim and it has masses at the hip and feet. It is assumed that the heel strike is inelastic so there would be no bounce off the surface and the foot acts like a hinge while remaining on the ground until the swing foot reaches its heel strike. There is only one foot on the surface at a time, and to avoid foot scuffing the swing foot briefly passes through the surface when the stance leg is near vertical. McGeer's and Garcia's PDWs are shown in Figure 2.2.

Various other walkers and models have been developed since McGeer's prototype, with some researchers utilizing tinker toys for their initial findings. Coleman and Ruina [7] constructed an uncontrolled walking toy (see Figure 2.4) that was statically unstable in all standing positions, but stable in motion. Wu and Sabet [48] built a similar straight-legged tinker toy (see Figure 2.5)

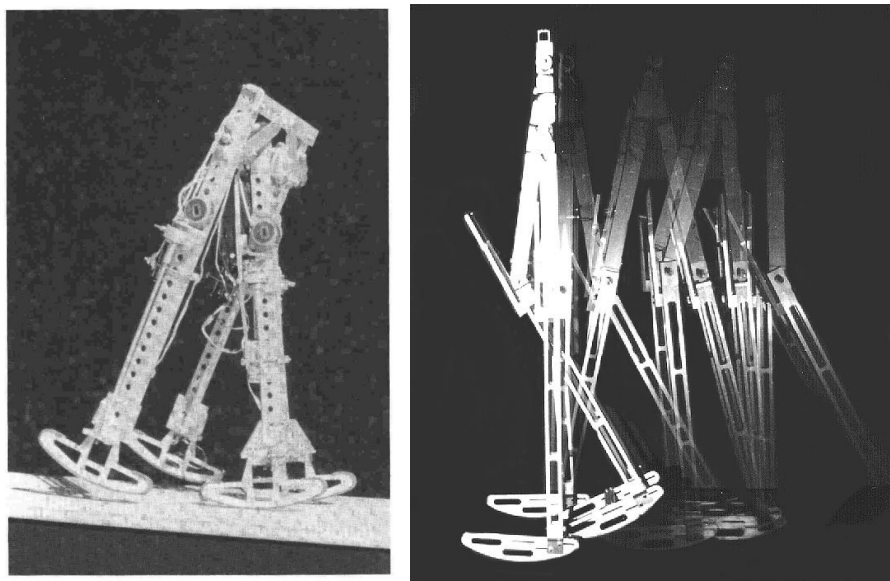


Figure 2.2: McGeer prototype and Cornell version with knees

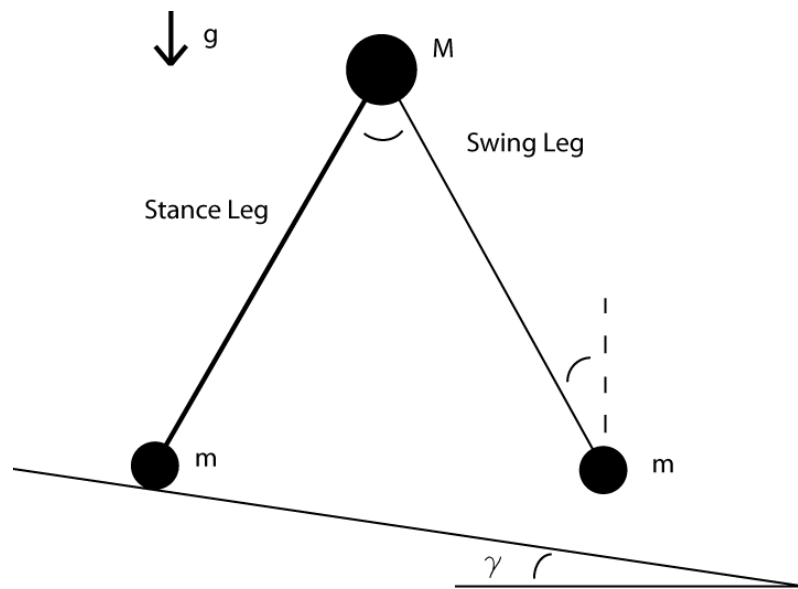


Figure 2.3: Garcia et al. point foot model that assumes $M \gg m$

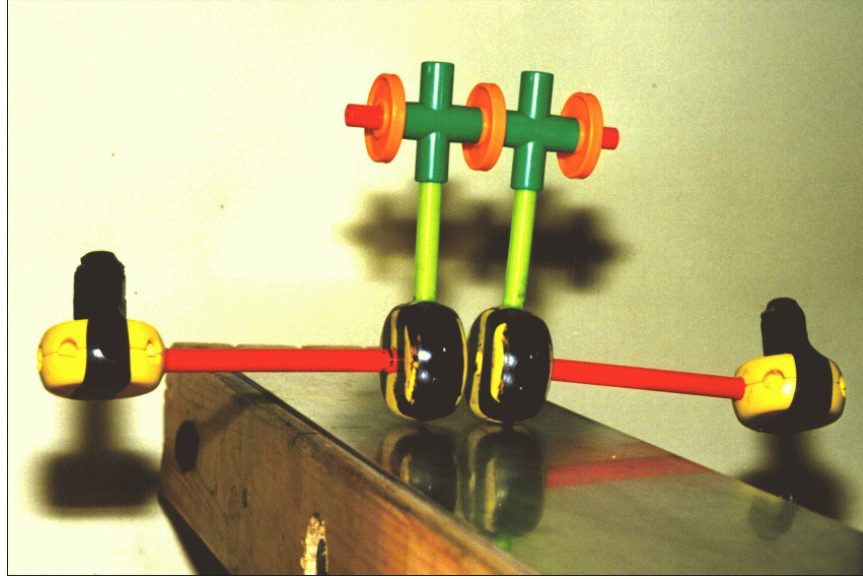


Figure 2.4: Coleman and Ruina tinker toy

with flat feet to study the size of the flat feet on gait patterns, friction between the ramp and feet, and the effects of ramp angles. Honeycutt [20] constructed a tinker toy (see Figure 2.6) using the exact design specifications given by Coleman and made an angle finder for the weighs of the walker.

Similar in simplicity of design to a tinker toy, Tedrake et al. [43] actuated a simple 3D passive dynamic walker by adding two active joints at each ankle and keeping the hip joint passive. With adding the active joints, the robot was able to walk on flat terrain and up a small slope (see Figure 2.7).

Wissem and Linde created a version of McGeer's straight-legged passive dynamic prototype. This version did not have feet, nor did it require actuation walking on stepping tiles. Wissem and Linde [47] also created a humanoid-looking walker topologically identical with the exception of a mechanism that lifts the middle foot during the swing phase that allows the PDW to walk without floor tiles (see Figure 2.8).

Collins et al. [8] built the first three-dimensional, kneeled, two-legged, passive-dynamic walking machine. The walker contained counter-swinging arms that attached rigidly to their opposing legs. This walker had a leg length of 85 cm and weighed 4.8 kg (see Figure 2.9).



Figure 2.5: Wu and Sabet tinker toy

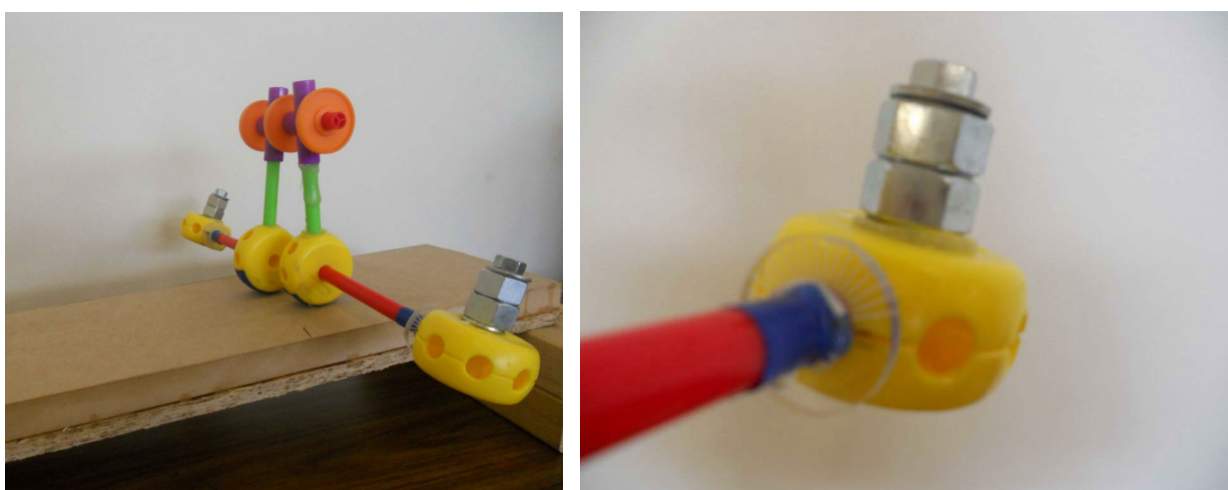


Figure 2.6: Honeycutt tinker toy and angle finder

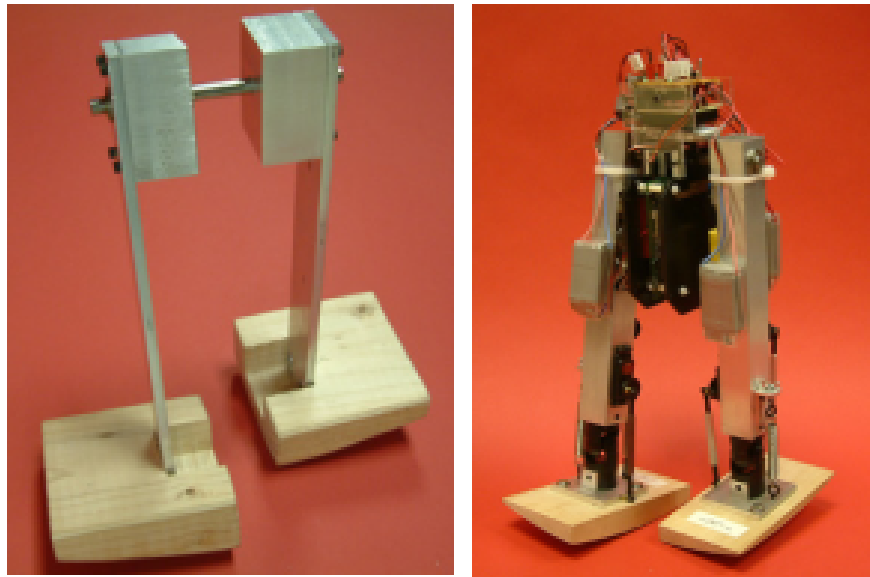


Figure 2.7: Toddler robot before and after actuation by Tedrake et al.

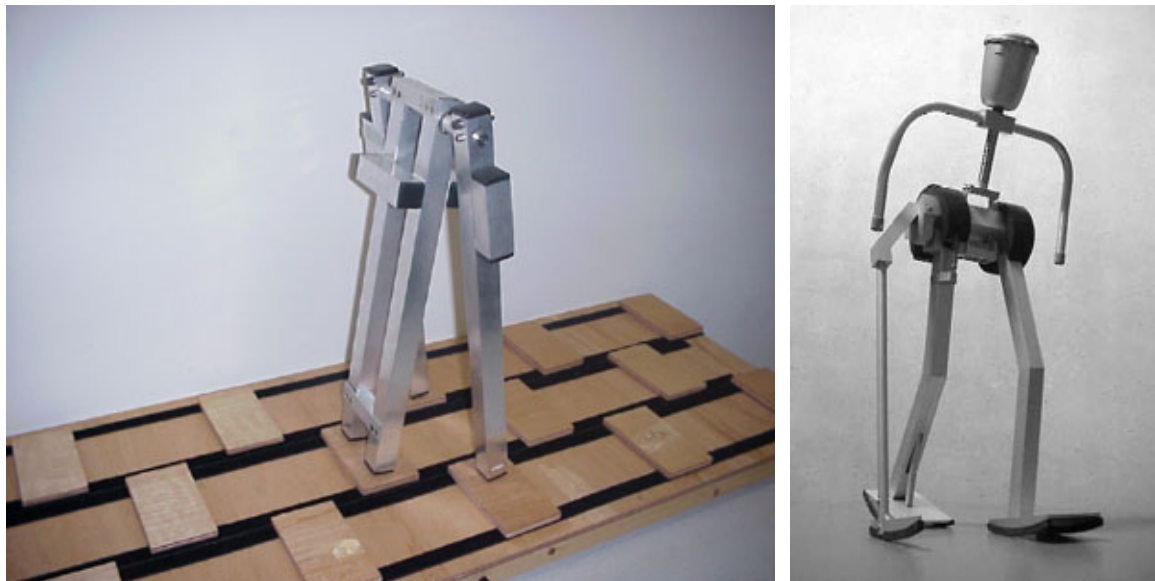


Figure 2.8: Version of McGeer's PDW without feet and Museon



Figure 2.9: Two legged two kneed PDW with arms

Trifonov and Hashimoto [44] built a walker 89 cm in length with a total mass of 4.5 kg (see Figure 2.10). This PDW was used to compare different designs of knee-locking mechanisms. With the active lock release, the number of steps taken was somewhat uniform and completed up to seven steps. The magnetic release achieved up to five steps seven percent of the time.

Chen [4] modeled and developed a PDW that featured electromagnetic clutches and suction cups for additional knee stability, thus preventing the knees from hyper-extending (see Figure 2.11). Chen modeled the two-link stance phase and three-link stance phase for a kneed PDW as seen in the introduction. The knee strike and heel strike events were modeled as instantaneous inelastic collisions. The upper portion of Chen's walker had a mass of 0.491 kg and the lower legs were about a forth of the mass of the upper section.

Honeycutt [20] furthered Chen's model by differentiating between each leg of a PDW. Sushko [42] then advanced the model by adding masses to better define the mass distribution of a PDW. In addition to the model, Honeycutt built a PDW (see Figure 2.12) that weighed almost



Figure 2.10: Trifonov and Hashimoto PDW



Figure 2.11: Chen PDW



Figure 2.12: Honeycutt PDW

seven kilograms using a latch mechanism for locking the knees using DC motors. The latches unlocked at heel strike events.

In 2006, Nagoya Institute of Technology [21] built a 0.42-meter long, 1.5 kg completely passive walker (see Figure 2.13). This PDW had a sixty percent success rate on a ramp with a stopper to maintain constant inter-leg angle. In experimenting on a treadmill, on a launch the walker achieved 4010 continuous steps.

In 2010, Koop [24] from the University of Manitoba built Dexter III (see Figure 2.14) and achieved over 1500 steps [28] on a single run. Using Dexter III, Rushdi et al. [39] found that testing on a treadmill was equivalent to testing on a ramp. Dexter III is 54.62 cm in length and weighs 8.72 kg.

In 2013, Koop and Wu [25] constructed Hip Mass 2 Links (HM2L) in order to validate their proposed model using the Hunt-Crossley contact model, and the LuGre friction model to represent



Figure 2.13: Nagoya PDW

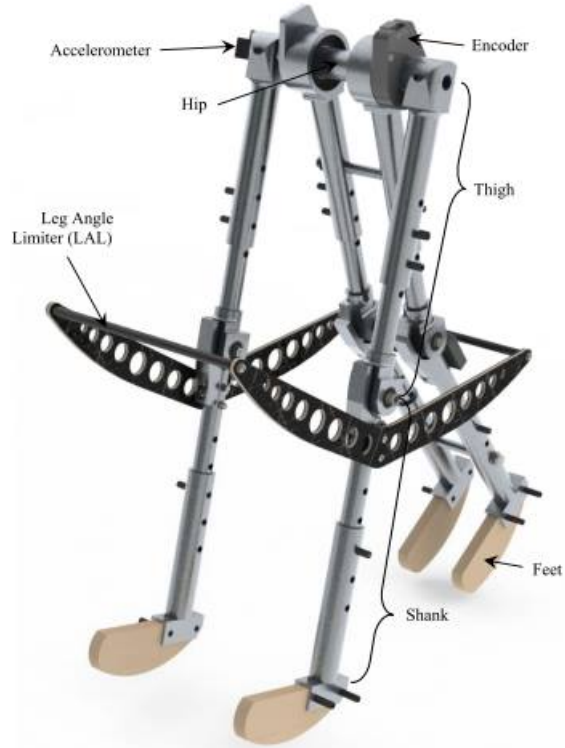


Figure 2.14: Dexter III

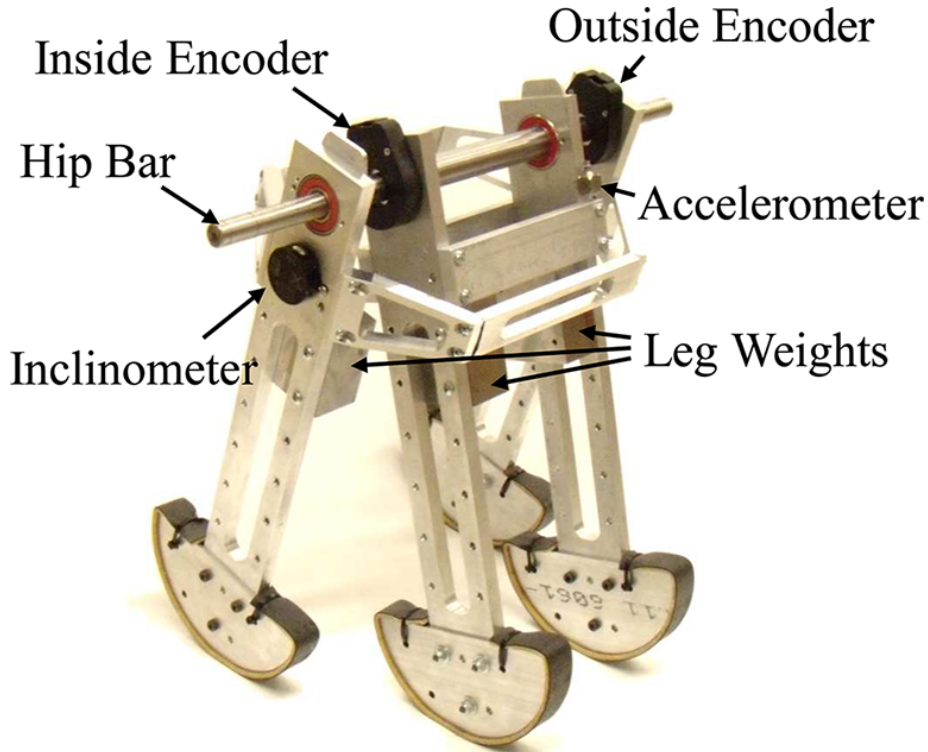


Figure 2.15: HM2L

the normal and tangential ground reactions. HM2L is compact and robust weighing 11.595 kg with a walker height of 40.64 cm (see Figure 2.15).

2.2 PDW Consistency

While varieties of walkers have been produced, there has been minimal discussion on issues and the consistency of these mechanical systems. Walkers with leg lengths comparable to adult humans have not displayed the same reliability of their more compact counterparts. Collins et al. [8] stated that “on a good day and with a practiced hand,” their “passive walker walks steadily in about 80% of launches” and that inappropriate initial conditions were the primary cause of failed launches. Chen’s walker “would take 3-4 steps before falling,” but no percent of successful launches were given. Trifonov and Hashimoto [44] stated that out of a hundred trials their walker “achieved an average of forty-four successful walks with” their active release system and achieved seven for their magnetic approach. Trifonov and Hashimoto’s determination of successful runs

were if the PDW took five or more steps. Using a tinker toy, Wu and Sabet [48] were able to achieve between a 70%-80% successful launch rate and were able to achieve more than 90% after several trials. Using Dexter III, Rushdi et al [39], as previously stated, achieved 1500 steps without falling on a launch but completed an average of between 9-18 steps with varying treadmill angles. The most reliable walker known to the author is from the Nagoya Institute of Technology [21] that walked up to eight steps with about a 60% success rate on a ramp with a stopper, but no data is given of the average number of steps at or above eight. Without a stopper the walker never achieved eight steps.

2.3 Model Evolution

Computer simulations have also evolved since McGeer's initial models. The compass gait model, which is an inverted double pendulum with two leg masses and a hip mass [10], was developed to include a full mathematical model with knees by Chen [4]. Honeycutt et al. [19] further developed the model differentiating the left and right legs while Sushko [42] added an additional mass to each limb. Honeycutt modeled how different asymmetric gait patterns arose due to specific changes in the physical parameters. The parameters changed were the mass of the thigh, mass of the shank, location of the knee, mass location of the thigh, mass location of the shank, and total length of the leg. From changing those parameters, they found four step patterns: symmetric single step, leg specific single step, leg specific double step, and leg specific quadruple step. This model is the first to the author's knowledge of a model looking at asymmetry in passive dynamic walkers. See Figure 2.16 for a evolution of the PDW model.

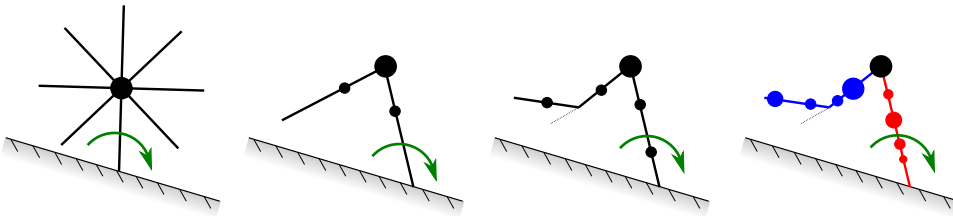


Figure 2.16: PDW evolution. (Left-Right rimless wheel, compass gait, 5 mass compass gait, 9 mass compass gait)

Although not often displayed as important, one factor for PDWs is the roll over shape (ROS). This shape (or radius) affects a PDW's balance and control. McGeer showed through design trials that 1/3 of the total leg length [32] is theoretically the most effective foot radius, which approximately matches the human ROS [1]. Handzic [14], furthered Honeycutt et al.'s work by incorporating the foot shape and did not limit the PDW to only a constant ROS [14]. In humans, Adamczyk et al. found that the net metabolic rate decreased with an increased arc radius to a minimum at 0.3 of the leg length. In other words, with a foot curvature of 30% the leg length is energetically advantageous partially due to the decreased work for step-to-step transitions. Other models have been developed, but for simplicity are not mentioned as they were not used in this experiment.

When developing a model there are a few assumptions that are commonly used. One such assumption is of frictionless hip and knees. This simplifies the mathematical models so that energy is conserved. If damping is not minimal then the PDW will not be successful in walking. Another assumption is that the hip mass is much greater than the mass of the foot. If this were not the case, the swing motion would affect the motion of the hip. The third assumption is that there is no bounce at the knee or heel strike events. These events are determined to be inelastic so that the foot remains on the ground.

2.4 3D Printing

Over a little more than the last ten years, 3D printers have steadily decreased in price with professional printers once costing \$45,000, now costing less than \$10,000 [23] and do-it-yourself kits under \$500. The market is estimated to have surpassed \$3 billion in 2014 [22] worldwide. It is estimated that the medical 3D printing market will reach \$983.2 million by the year 2020 [9]. 3D printing is very broad as printers are able to utilize metals, polymers, ceramics [22] and human tissue [12] to build. In the health care industry, organizations such as e-NABLE have made a 3D printed plastic hand that cost \$50. Commercially made prosthetics can range from \$30,000-\$50,000 [28]. Prosthetics are not one size fits all, but with the ease and speed of designing and

modifying products these items are built economically with 3D printers using plastic. Although there is a stark difference in price, this does not mean that the products are equal in quality. Some advantages and disadvantages of 3D printing are listed in Table 2.1.

Table 2.1: Advantages and disadvantages of 3D printing

Advantages	Disadvantages
Automated Process	Reduced choice of materials and colors
No need for costly tools, molds, or punches	Lower precision relative to other technologies
Minor or no finishing required	Limited strength
Modification of internal geometries	-

Currently, the primary use of 3D printing is to manufacture prototypes. Items that are to be metal can be produced using plastic in the developmental stage while also varying the size. Without the need for costly tools or molds, savings is accrued along with increased security and privacy if produced in-house [3]. When altering internal geometries, designers are able to produce items that are unable to be manufactured using any other manufacturing processes. An example of this is GE's Leap engine fuel nozzle [49].

Chapter 3: LUIGI

3.1 Body Construction

As previously stated, the design of LUIGI (see Figure 3.1) came from the University of Manitoba. The design was sought due to its past performance. Design lengths remained constant and 3D printing was utilized to lighten the walker. It is known that having the hip mass greater than the foot mass is put into practice so the swing motion does not affect the motion of the hip, and Chyou et al. [6] showed that adding a torso to a PDW improved stability and walking speed. Therefore, lightening the lower portion of LUIGI was the focus of change for material. A few components were combined into an assembly and others were modified for simplicity.

Dexter III's upper thighs are made from one piece of aluminum, but LUIGI's are divided into two different pieces: cap and body. Instead of the need to manufacture the parts from a block of aluminum, they were now made with tubing and a printed cap. The cap connected to the hip was printed using acrylonitrile butadiene styrene (ABS), and depending on if it was the inner or outer thigh, the hole was drilled to size for a press fit with the bearings or to the hip itself. An extension on the bottom of the caps was inserted into the tubing for a friction fit. The back portion of the inner thigh was adjusted because no encoder or accelerometer was to be used in testing. Figure 3.2 displays the new and old thigh components.

LUIGI's shin shank is a combination of the patella, knee connector and the shank for the shin of Dexter III (see Figure 3.3). Joining the three pieces into one eliminates the need for nut and bolt, which are made from steel. Steel is denser than aluminum, and thus the removal of it from the walker is vital in reducing its mass. The area of the patella that housed the bolt was filled in to reduce geometric complexities and any stress concentrations.

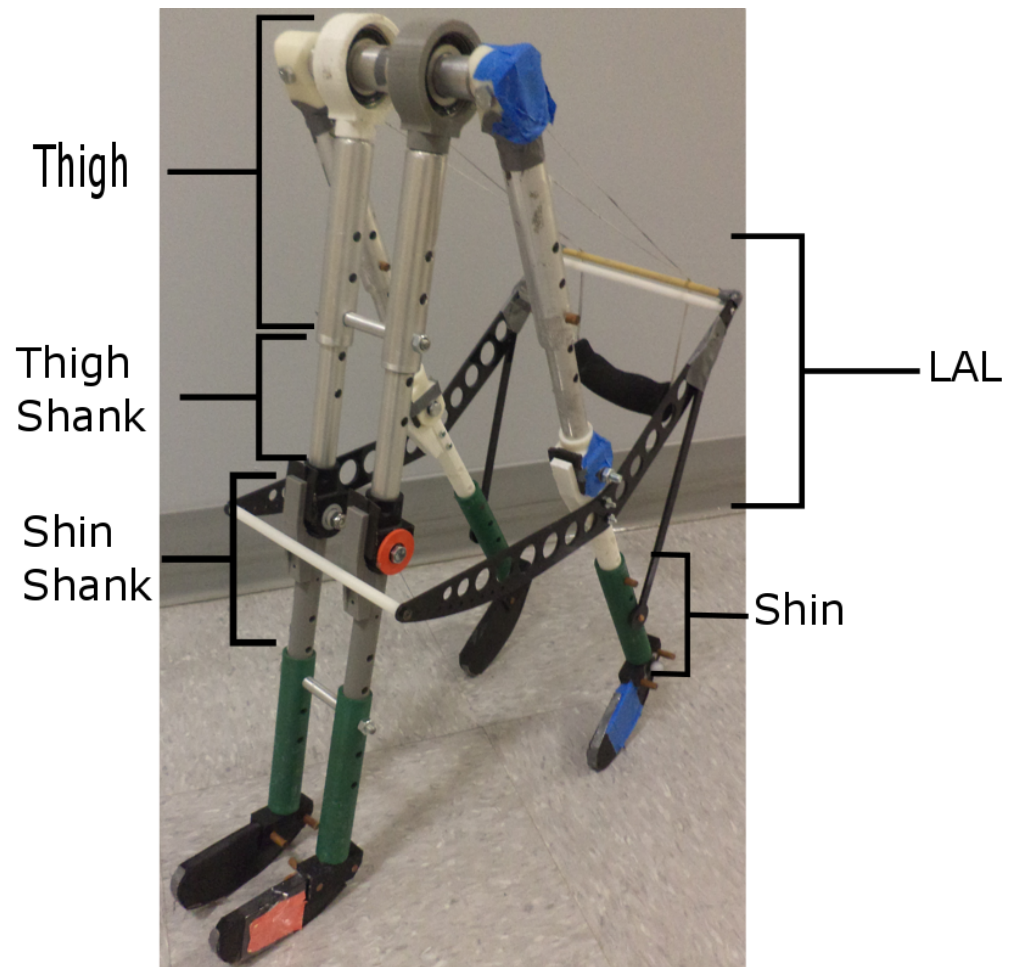


Figure 3.1: LUIGI, based on Dexter III

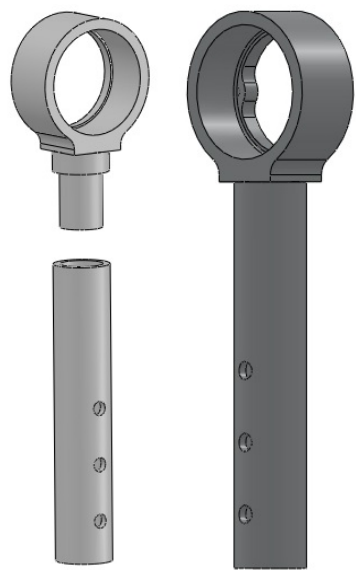


Figure 3.2: PDW thigh comparison. (Left) LUIGI thigh and (Right) Dexter III thigh

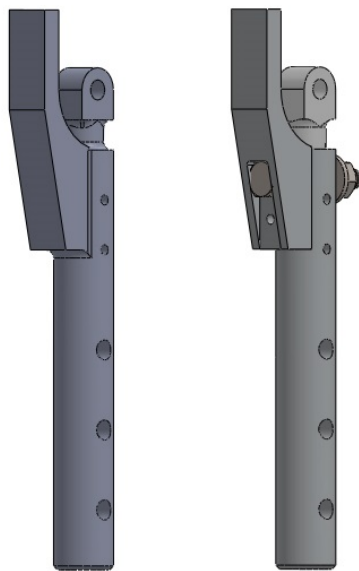


Figure 3.3: PDW shank comparison. (Left) LUIGI shank and (Right) Dexter III shank assembly

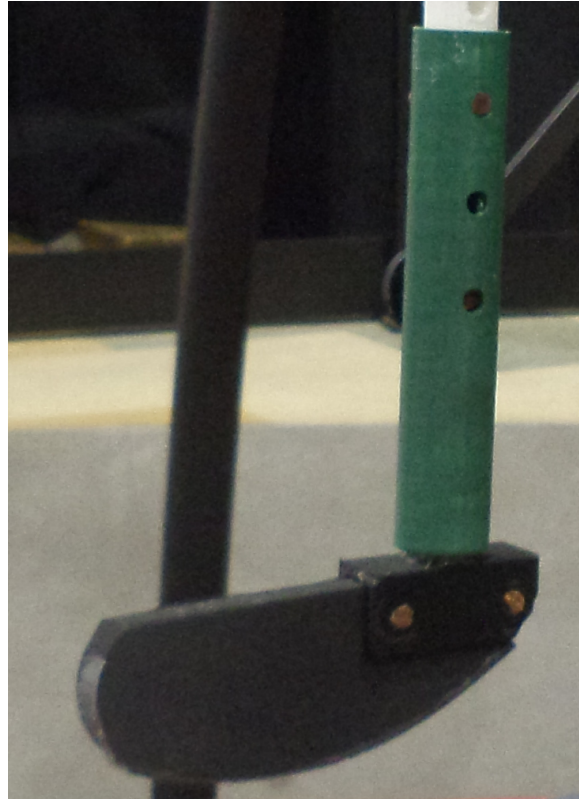


Figure 3.4: Foot, foot bracket and shin of LUIGI made with ABS

The knee joint, shin, and foot bracket, which is aluminum on Dexter III, were printed using ABS for LUIGI (see Figure 3.4). The foot, which was wood on Dexter III, was also printed with ABS. Another minor modification was the addition of padding to the bottom of the feet for grip.

ABS was used for strength, but issues arose when printing pieces of higher complexity or greater size. **Polyalctic acid (PLA) was then used because it does not require a headed plate to promote adhesion or prevent thermal curling** [13]. The printers used were the **MakerBot Replicator 2X** for printing with ABS and the **MakerBot Replicator Z18** for printing with PLA. According to the Material Safety Data Sheets from the supplier, the density of the **PLA** is **1.24 g/cm³**, and the **ABS** ranges from **1.03-1.10 g/cm³**. There is variance of percent fill for each component as some pieces, such as the **feet**, were printed at a very low percent fill (**5%**), while the **hip caps** (**60%-70% fill**) were higher due to drilling out holes for press fits. A higher fill for the caps was required for a greater frictional area. The number of shells was two for all parts, but the percent fill ranged

from 5%-70%. Certain pieces were modified to have a smaller diameter but were then reamed to the desired size. Completely closing openings would have wasted more material and resulted in longer print times.

3.2 Other Components

Metal pins used to connect components for Dexter III were replaced with wood dowel rods. The leg angle limiter (LAL) panels, which for Dexter III were carbon fiber with balsa wood core and aluminum inserts, are acetal homopolymer resin for LUIGI. The bar which separates the LAL rod is acetal. LUIGI also utilizes a smaller bolt size (1/8 inch) on the LAL panel, which connects to the shank.

Chapter 4: Simulation Data

4.1 Mass Moment of Inertia

For the MATLAB simulation the mass moment of inertia, damping of the hip and knee bearings and the foot shape were all required inputs. Individual components were weighted and computer aided drawing (CAD) density properties were adjusted to reflect the physical components. Afterwards, the mass moment of inertia of four assemblies; inner thigh assembly, outer thigh assembly, inner shin assembly, and outer shin assembly were found.

4.2 Damping

Damping from the hip and knee bearings were found by utilizing the Computer Assisted Rehabilitation Environment (CAREN) System. With knowledge of the x, y, z coordinate system, experiments were conducted with aligning test components in a plane (see Figures 4.1 and 4.2 for test setups).

Two motion capture nodes were put on the limb, one at the center of rotation and the other at the opposing end. For testing of the hip, the limb was raised until it was approximately parallel with the holding block and then released. Following the release, the x, y, and z coordinates for the two nodes as well as a time stamp would be recorded until the limb stopped moving. The side-shields of the hip bearings were removed and were tested with and without WD-40 to see the impact on damping. Two different knee bearings were tested: stainless steel, double-sealed ball bearings and lubrication-free acetal ball bearings. No additional lubrication was added to the knee bearings due to their accessibility on the walker (see Table 4.1 for results).

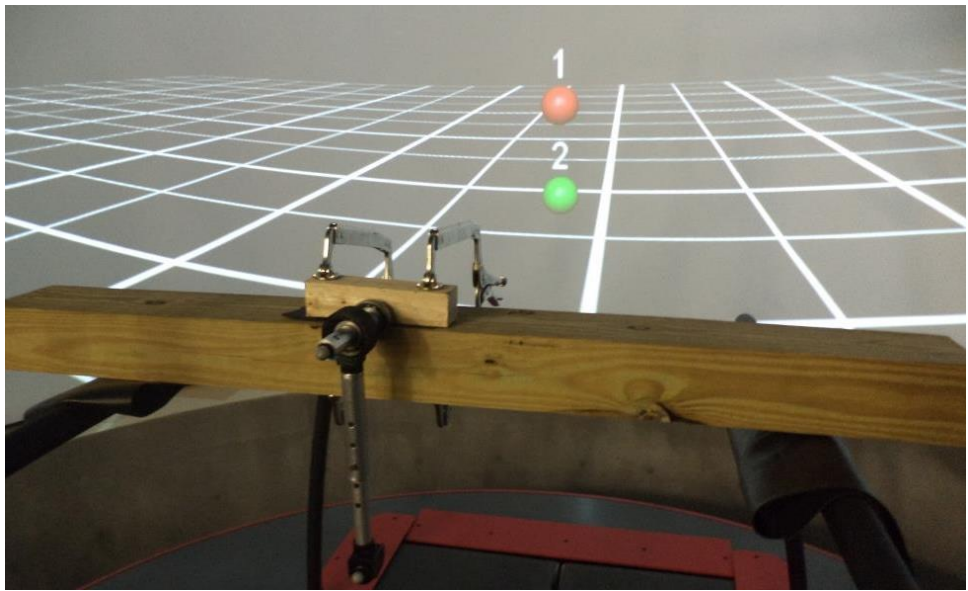


Figure 4.1: Hip damping setup on the CAREN system



Figure 4.2: Knee damping setup on the CAREN system

Once data was collected, processing was done using MATLAB. The first and last 20% of data were cut off. This was done to analyze damping at a steady state. The time readings were subtracted by the initial time for the time stamp. For each marker (1 and 2), their respective coordinates were assigned to a vector, and the differences between marker positions were found. The angle of rotation for the limb was found as the inverse tangent of the change in x divided by the change in y. This formula changed to dz/dy when calculating damping of the knee. Peaks were found using the findpeaks function in MATLAB, and the logarithmic decrement and damping coefficient were calculated. The logarithmic decrement was found with:

$$\delta = \frac{1}{n} \log\left(\frac{x_0}{x_i}\right)$$

where,

n = Peak index minus one

x_0 = Initial peak value

x_i = Peak index

The damping coefficient was found as:

$$\zeta = \frac{1}{\sqrt[2]{1 + 2\pi/\delta^2}}$$

Once a damping coefficient was calculated along the entirety of the experiment, the average was taken. To find the damping constant C, the peak number and difference from the initial peak time and final peak time was calculated. Then the damping frequency was found by finding the number of peaks divided by the time. The natural damping frequency was found by multiplying 2 times pi by the damping frequency. The natural frequency was calculated by:

$$f = \frac{f_n}{\sqrt[2]{(1 - \zeta_a v_g)}}$$

where,

$$f_n = \text{Natural damping frequency}$$
$$\zeta_a = \text{Average damping coefficient}$$

Finally the **damping constant** C was found using:

$$C = 2\zeta_a f$$

Table 4.1: Experimentally found damping values with data from the CAREN system

-	Damping Coefficient	Damping Constant
Single Hip	0.0136433	0.195536
Double Hip	0.0131227	0.200936
Single Hip with Lubricant	0.00768207	0.107884
Double Hip with Lubricant	0.00642269	0.0912232
Steel Knee Bearing	0.0118029	0.189182
Acetal Knee Bearing	0.00276516	0.0399635

The single hip and double hip were very similar as were the respective hips with lubricant as they should be. Knee damping was starkly different as the acetal bearing were five times smaller than the steel knee bearing.

4.3 Foot Shape

The foot shape did not require calculations as the shape has a constant radius with an offset. Although as previously noted of the theoretically optimized foot shape being one-third the leg length, Dexter III used a radius of about two-tenths of the leg length (see Figure 4.3).

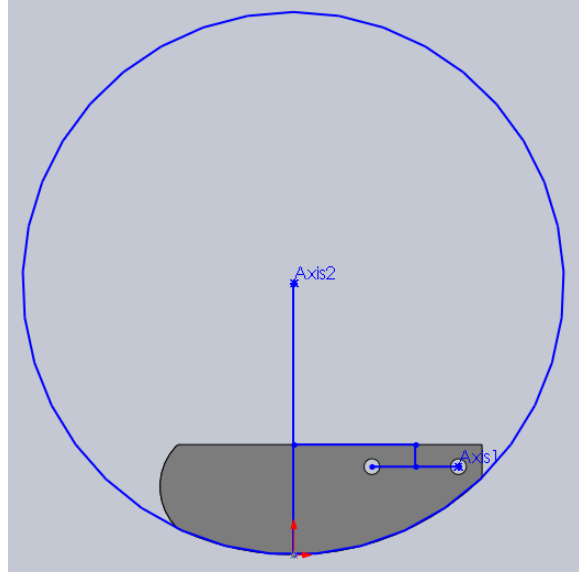


Figure 4.3: CAD rendering of foot with circle to show the constant radius

4.4 Testing Parameters

From the work of Sushko [42] [41], the parameters to alter are the added mass, the added mass location, and the mass of the hip. The added mass and added mass locations are for each limb. The possible lengths examined were kept to three. The length test points ranged from the origin to the usable length of the limb. For instance, the full length of the thigh encompasses the knee joint (see Figure 4.4), but adding a mass to the joint is not possible due to its geometry. Thereby, the three points were: at the center of rotation, the usable length, and the midpoint point between said points.

The mass variance was kept to at least four (five for the hip), beginning with no mass added up to a given maximum. These varied based off the component with the hip mass having the most weight to have added. The maximum given for masses was determined based on the number of possible weights that could fit for a point load. Masses used were 4-ounce lead weights that were wrapped around each other and onto the limb using clay and tape (see Figure 4.5).

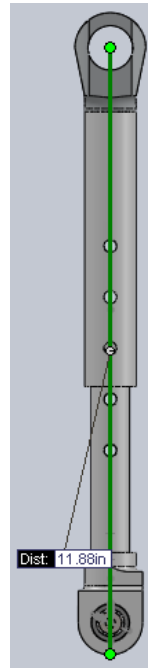


Figure 4.4: Total length of the upper inner thigh



Figure 4.5: Example of the attachment of weights on LUIGI

Chapter 5: Results

The goals of this study were to verify the asymmetric walking model, improve consistency of successful runs, and proof of concept for 3D printing. Through experimentation of differing launch scenarios consistency of the LUIGI was established and showed which weight placements improved reliability. Although never reaching a steady state in any launches, 3D printing had success and achieved five steps. This success is comparable to previously built passive dynamic walkers.

5.1 Prior to Simulation

Testing was conducted on a previously built ramp. A hand-held tether was secured to LUIGI to ensure it would not topple completely when falling. Through preliminary observation of the swing motion of the legs, it was determined to use wooden blocks for the walker to step on. This was due to little to no observable bending of the knee while swinging at rest. Without sufficient flexure of the limb, the walker will scuff its feet on the ramp while walking and trip.

A variety of leg angles were used in the launches to determine optimal angles to use during testing as well as give an idea of angles to use for the simulation. When launching, the inner legs were released from a state of rest. This was to assist with making launches easily repeatable.

During this time, LUIGI completed four steps multiple times. Through these tests, it was estimated that the successful position of the inner legs were between zero and five degrees, and the outer legs were optimal at approximately forty five degrees for the three degree ramp slope. See Figure 5.1 for a example launch setup.

With having successful runs, testing was conducted to eliminate the stepping blocks. The first tests were having each step block decrease in height, beginning with a half inch down to no



Figure 5.1: Launcher setup to remove human variability

block in quarter increments. LUIGI had a 6%-9% success rate of walking on stepping blocks that were a quarter inch smaller than the previous step. Another test was for LUIGI to initially start from a block then step to the ramp but success remained limited.

5.2 Simulation with No Weight

When simulating LUIGI with its mass moment of inertia values and given release angles the walker would fall before achieving a stable gait. A stable gait in the program is taking at least 20 strides. One stride equaled a step with both left and right legs. However, when the inner legs release angle was lowered the run was successful. Based off the simulation results (see Table 5.1), LUIGI without any masses had a step length asymmetry of 25.332% and a swing time asymmetry of 16.511%. Asymmetry is calculated by taking the absolute value of the difference in value of the left and right legs and dividing that by the average of both leg values.

$$\% \text{Asymmetry} = \frac{|L_a - R_a|}{\frac{L_a + R_a}{2}}$$

where,

L_a = Left leg average

R_a = Right leg average

Table 5.1: Steady state gait with no weight added simulation results from MATLAB for LUIGI

Variable	Result
Average Left Step Length	0.287 m
Average Right Step Length	0.223 m
Step Length Asymmetry	25.332%
Average Left Swing Time	0.462 sec
Average Right Swing Time	0.545 sec
Swing Time Asymmetry	16.511%

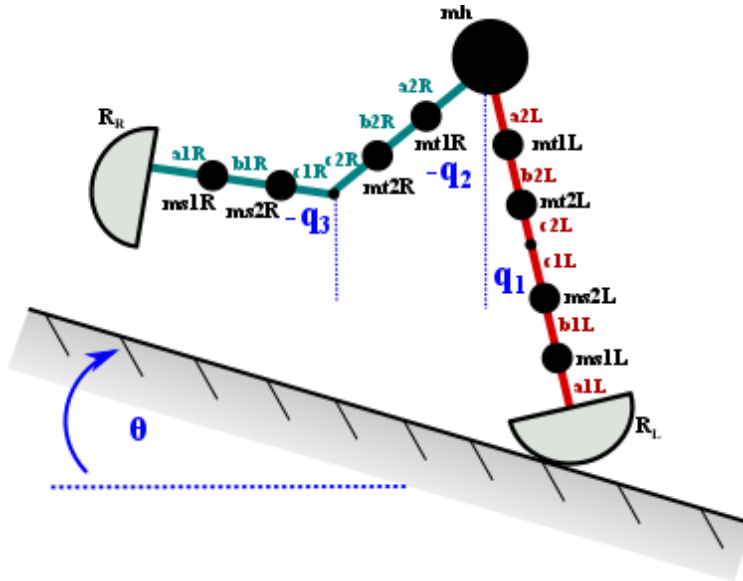


Figure 5.2: Breakdown of the 9 mass kneed walker model

Upon having the physical walker and model achieve successful runs, iteration of the simulation was conducted. After filtering out duplicate systems, the total number of simulations numbered 45,118 of which 30,833, (68.34%) had a stable gait. These simulations came from altering additional masses and its placement on the four limbs. In other words the model began as a five mass kneed walker model and had the potential to become a nine mass kneed walker (see Figure 5.2). Parameters that remained constant were the ramp angle, foot shape, initial velocities, and initial angles for the legs.

By going from a five mass model up to a nine mass model, a larger range of dynamics are possible can enable more symmetric versions of the gait and also more asymmetric versions of the gait. In other words by adding additional masses at locations specified by the simulation one

changes the original gait asymmetry (in this case 25%) to either a symmetric gait (0%-2%) or more asymmetric gait (40% or more). Both of these conditions will be examined below.

5.3 Symmetric (0% - 2%)

It was determined to see if the LUIGI could walk successfully with weights that in theory would give the walker a symmetric gait. Symmetry was limited to be between zero to two percent asymmetry. Out of all the 30,833 stable gait lengths, there were 784 that achieved the specified step length, and out of those 317 had the specified step time. Figure 5.3 is the graph of said symmetric systems with their percent asymmetry for step length and step time. Systems with added hip masses were noted and would eventually be tested due to their added stability over systems without added hip mass. Multiple systems were tested, and results were similar to that of the initial testing. The walker seemed more stable with an added hip mass, but issues arose with twisting of the foot bracket and thigh. Successful launches of the weight placement for symmetric gait were between 30%-40%.

5.4 Asymmetric Simulation (40% or More)

Asymmetry was limited to greater than or equal to forty percent of which only 76 systems (see Figure 5.4) out of the data were eligible. There is one point that extends to just over 60%, and it is the highest known point out of the data. Again, systems with added hip masses were preferred and tested. The physical results were not as successful as the symmetric weight placements. Successful launches of the weight placement for asymmetric gait ranged from 10%-20%. Two asymmetric systems in particular were tested and their values are listed in Table 5.2.

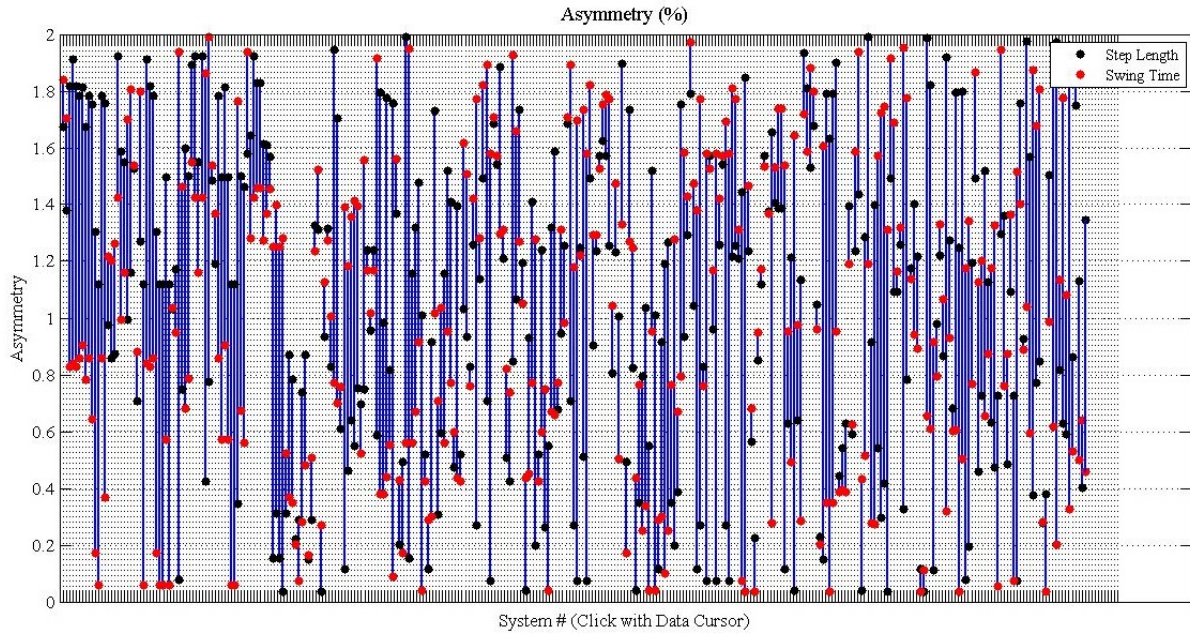


Figure 5.3: All 0% - 2% asymmetric systems from the simulation. Systems are on the x-axis with their asymmetric values on the y-axis. The simulation begins with the original 5 mass model and goes up to a 9 mass model thus changing the dynamics of the entire system and changing its asymmetrical values

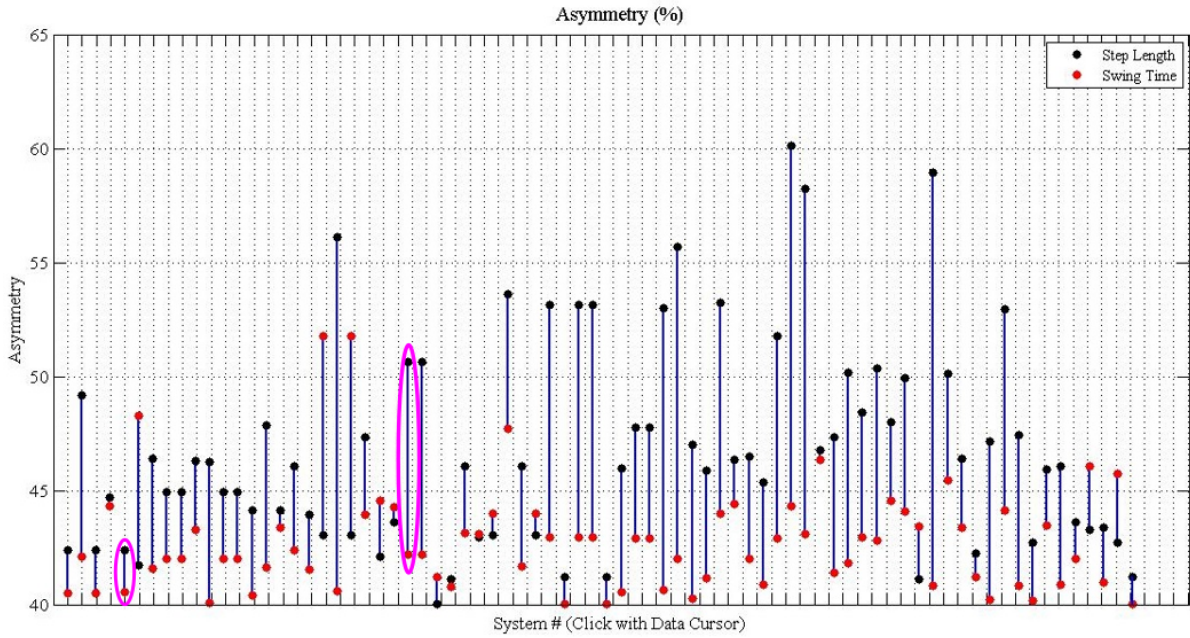


Figure 5.4: All 40% or more asymmetric systems from the simulation with trial systems highlighted. Systems are on the x-axis with their asymmetric values on the y-axis. The simulation begins with the original 5 mass model and goes up to a 9 mass model thus changing the dynamics of the entire system and changing its asymmetrical values

Table 5.2: Trial system's asymmetric gait simulation results as well as how much mass to add and where to achieve stated asymmetry

-	System A	System B
Step Length Asymmetry -	42.359% (L: 0.271 m, R: 0.176 m)	50.645% (L: 0.287 m, R: 0.171 m)
Step Time Asymmetry -	40.535% (L: 0.429 s, R: 0.647 s)	42.193% (L: 0.430 s, R: 0.660 s)
Additional Hip Mass	0.1722 kg (24.6 weights)	0.1722 kg (24.6 weights)
Additional Left Shin Mass	0.0547 kg (7.8 weights)	-
Additional Left Thigh Mass	0.1820 kg (26.0 weights)	0.1820 kg (26.0 weights)
Additional Right Shin Mass	0.0273 kg (3.9 weights)	0.0547 kg (7.8 weights)
q1	7 Degrees	7 Degrees
q2	-15 Degrees	-15 Degrees
q3	-16 Degrees	-16 Degrees

5.5 Asymmetric Physical Results

To compare with the simulation results, MATLAB was used to analyze the step lengths and times for the PDW in a video recording. This is possible with specifying a known distance and selecting frames in which heel strikes occur. The results are listed in Table 5.3.

Table 5.3: Asymmetric gait results for LUIGI

Step	Step Time (s)	Step Length (cm) (
1	1.50	105.662
2	2.00	92.971
3	2.67	70.991
4	3.34	54.855
5	4.00	48.009

5.6 LUIGI Consistency

Successful launches for LUIGI varied depending on the experiment. Three primary tests were conducted following the computer simulation. The first being for the symmetric gait (0%-2% percent asymmetry) deemed by the program. The successful launches ranged between 30%-40% for this symmetric gait weight placement. Testing for asymmetry was about half with a range of

10%-20%. A third test placed weights evenly across the walker and had about the same success rate of the symmetric gait testing.

5.7 Additional Video Analysis

Four trials were chosen to graph angular position, angular velocity, and angular acceleration for the thigh and shin. These trials were recorded and then filtered using MATLAB. The trials differed in either setup or weight distribution. The weight configuration for trial one (Figure 5.5) was of System B, and the walker began from a stepping block directly to the ramp. Trial two (Figure 5.6) was a typical walking setup with blocks with the System B configuration. Trial three (Figure 5.7) consisted of the System B configuration going from the ramp to blocks. Finally, trial four (Figure 5.8) is of System A with the same initial conditions as trial one.

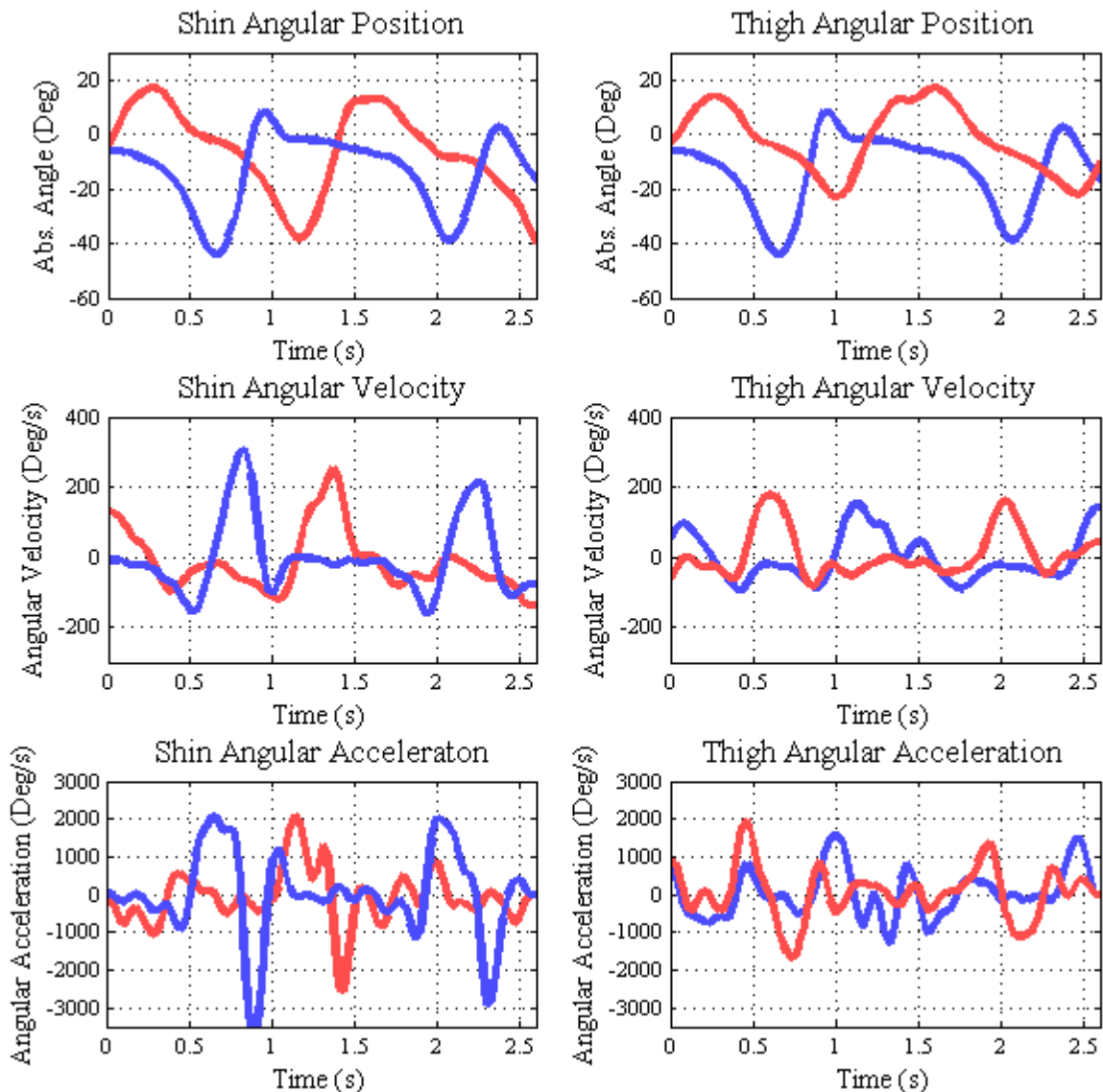


Figure 5.5: Trial 1 angular position, angular velocity, and angular acceleration for the shin and thigh

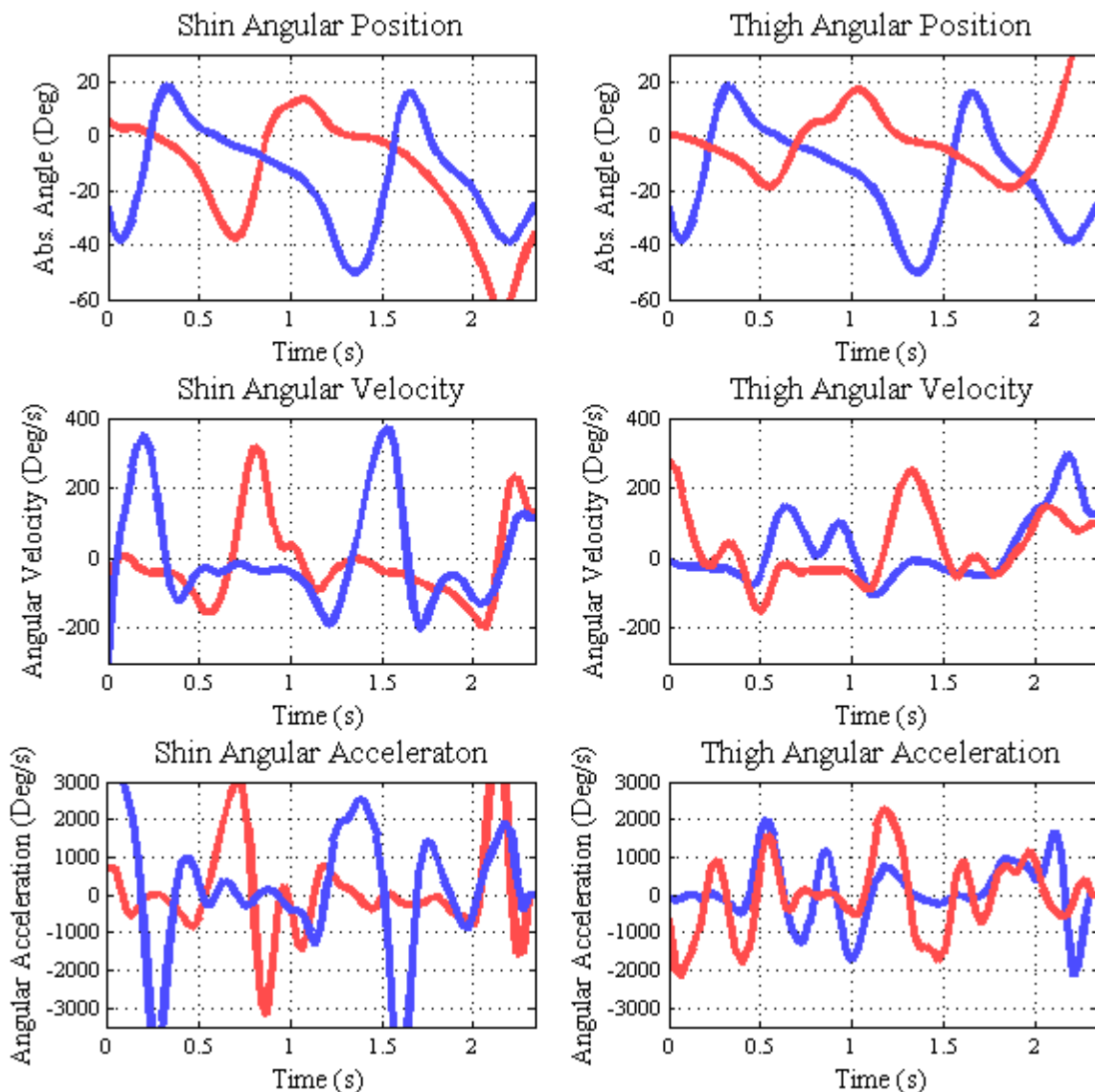


Figure 5.6: Trial 2 angular position, angular velocity, and angular acceleration for the shin and thigh

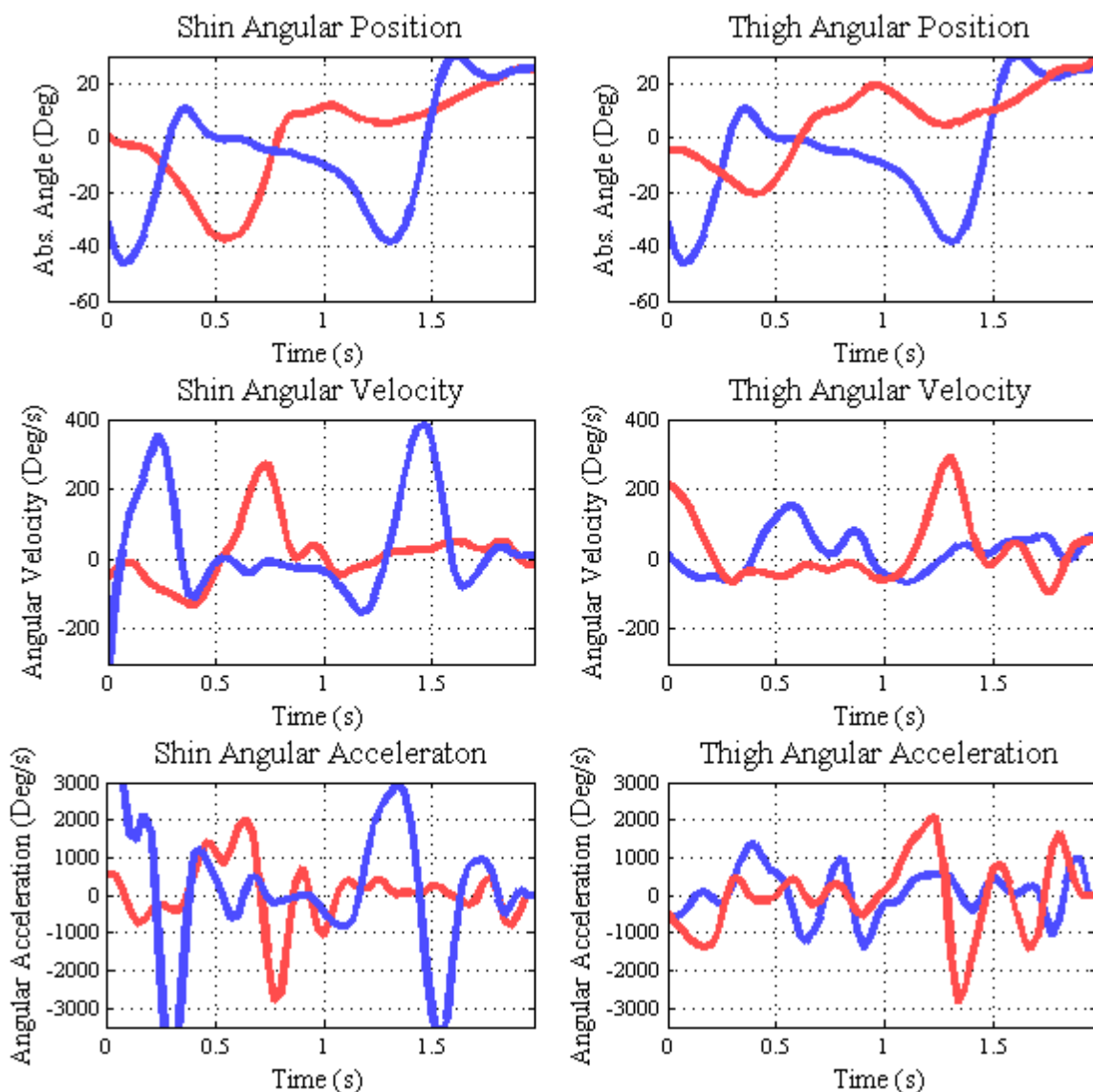


Figure 5.7: Trial 3 angular position, angular velocity, and angular acceleration for the shin and thigh

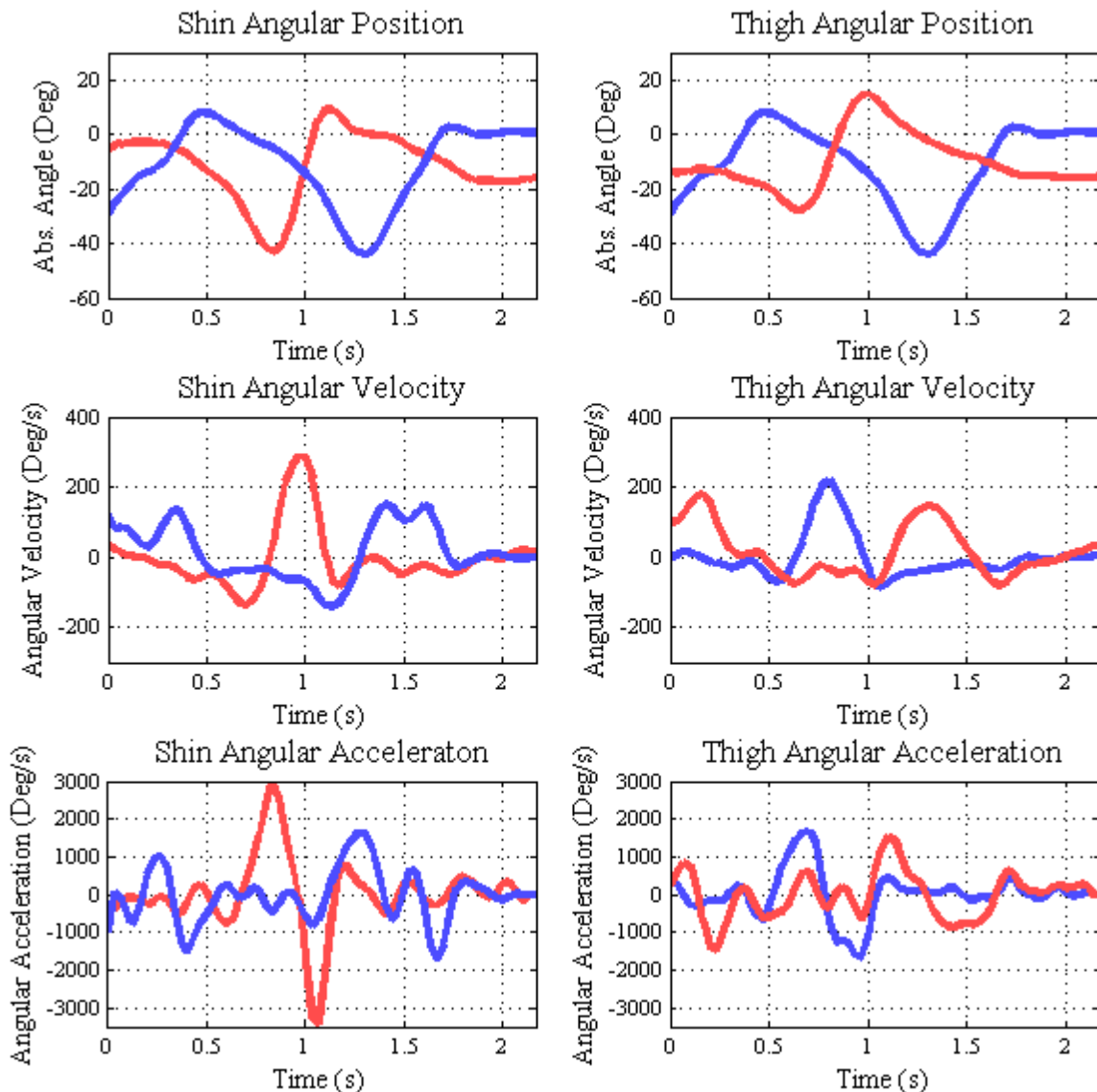


Figure 5.8: Trial 4 angular position, angular velocity, and angular acceleration for the shin and thigh

Chapter 6: Discussion/Conclusions

LUIGI, while based off a previous walker, has its own distinct features. It achieved a lightweight design and numerous successful runs, but it did not complete enough steps to display a steady gait. **LUIGI is the first successful walker to use additive manufacturing and is the only walker known to the author that meshes differing materials for the leg pieces.** As previously stated, obtaining **4-5 steps is a small success, but it does not suffice in providing the minimal amount of data to compare to the simulated model.** At a minimum, an average of 10 steps is required to ascertain similarities or differences. With that, the first two and last two steps could be omitted and the rest would be assumed to be at a steady state. Without having more steps it cannot be truly stated that the PDW came to an equilibrium in stability. From the asymmetric gait weight placement studied, LUIGI displayed a gradual decrease of step length.

There were a few differences between the model simulation and the physical walker. The model contained initial velocities, which is a reason why the angles differed from the physical results. Initial velocity could have been given to the walker, but that would have complicated launching and made it less easily repeatable. The model used calculated damping values, but the knee damping is not as accurate as the hip damping. The reason being is that **the thighs were pressed on to the bearing or to the hip, while the knees used a bolt to attach the knee joint to the lower section of the leg.** **If the bolt is tight, it could increase the damping, and if it is too little, had a danger to fall out while the walker was in motion.** Assuming inelastic collisions for the knee and heel strike events may not be an accurate assumption with LUIGI. Masses added to LUIGI were not exact to that of the model as they were rounded to the nearest whole value for number of pieces. Also, the tape and clay used to secure the walker was not taken into account. When using only tape or clay to secure the lead weights they would fall off during experiments.

With looking at the four videos for angular data, angular positions stayed relatively constant as can be seen in Figures 5.5, 5.6, 5.7, and 5.8. Again, if more steps were taken it would more reasonable to delve deeper in finding a connection, since the assumption could then be made that the system was at steady state. The Figures 5.5, 5.6, and 5.7 which are all of System B are similar. The velocities and accelerations are not as smooth in transitioning from one leg to another with jolts which could be indicated from the knee or heel strike collision events. Experimentation of the varied knee stoppers were used for LUIGI, but none displayed much difference from another. The primary stopper used was foam one-eighth in depth. Varying thicknesses and foams with different stiffness were used, but no noticeable difference was observed. The reason why there are multiple videos for the angular data compared to step length and step time is that the angular data do not require the heel strike events to be on the screen. HM2L displayed an inner leg angle that ranged from approximately one half to negative four fifths radians and displayed a constant frequency of position. This difference between the two PDWs could be from LUIGI being tested from asymmetric gait weight placement.

Out of all of the weight combinations, equal placement on each limb was slightly more reliable than the symmetric gait pattern, but there was some unsteadiness. Seemingly, the strength of the lower portion of the walker had difficulty in handling the added weight but said weight could have helped stabilize the knees. By increasing its inertia there could be less movement at heel or knee strike events. It is interesting to note the lower success rate for the asymmetric testing compared to the symmetric data. It is possible that having two different dynamic systems aids in instability and that could explain the greater number of symmetric systems found compared to asymmetric. From the randomized model, there were more than four times the amount of gait systems at the 0%-2% than for greater than 40% asymmetry. In an asymmetric system the hip moves at different speeds depending on which leg is in motion and will have more inertia than a symmetric system.

With the 3D printing, LUIGI is the lightest PDW but not the shortest. 3D printing had issues with larger size pieces. Visual inspection was done on all components to validate quality.

Even after passing the initial inspection connecting components together gave clues if something was off. Supports were used to reduce deformation on all pieces. It was better to have a lower percent fill on the knees to allow flexure when connecting to the thigh shank. By reducing infill to 20%, there were less brittle failures. The thigh caps needed to be a higher percent fill due to reaming out the holes but fracture did occur when attaching to the hip or bearings. Printing was done with the larger surface area on the build plate but hole integrity was decreased when there was noticeable movement between the hip and the hip bearing which was solved by reaming all holes. With all pieces, more than the required amounts needed were printed to account for failures. Printing the shin proved difficult, as it was not printed on its side. Printing with the opening on the print bed helped keep the integrity of the circle but as the print neared completion, it would fail more than half the time caused by separation of the piece from the building plate. If pieces were too large, sanding was done to reduce the size. Attempts to use a lathe to reduce the outer surface of a component were tested, but fracture occurred in two of the three efforts and was thus not reliable enough for production. The foot was printed on its top to keep integrity of the curvature of the part, but the bottom surface was not completely smooth. It seemed that preheating when printing ABS with these specific printers helped with reducing thermal gradients. Openings for bolts, dowel rods or knee joint seemed to be too small, whereas the hip holes were too large if printed to size.

Overall, 3D printing in the author's opinion would be better suited for a smaller, more robust PDW. Having the plastic inserted into the aluminum tubing would have worked much better than the reverse. For bearings, it was better for the plastic to enclose on the bearings than to insert the bearings into the plastic. Also, avoiding the use of steel nuts and bolts would improve the performance as it does not take much to over tighten and fracture plastic components. Optimal printing thickness was 0.2 mm since lower resolutions, although printed faster, did not have the precision needed and printing at a higher resolution resulted in failures due to deformation or clogging of the nozzle.

With the 3D printing, LUIGI is the lightest PDW but not the shortest. As compared to the Nagoya Institutes's most successful walker, LUIGI is approximately 12 cm taller and 100 grams

lighter. Compared to McGeer's LUIGI is 4 cm taller and more than half of the total mass of McGeer's walker. LUIGI is equal in length to that of Dexter III and taller than HM2L but has a fraction amount of mass relative to them. The lightweight features came at a cost of robustness, thus adding instability to the PDW.

6.1 Issues

There were a number of issues which plagued LUIGI. Using stepping-stones is not ideal as there placement may ruin a good release if one is out of place. This problem is greater for the outer legs as they need to hit instantaneously. A problem that compounded the footing was twisting of the foot bracket while walking. At times when a foot would hit the ramp or stepping block, one or more foot brackets would shift due to the force of contact. If the feet do not land at the same time, the walker will fall. Efforts were successful in mitigating the movement of the foot bracket but were never completely eliminated.

Twisting of the outer thighs would occur during the testing and when efforts were made to control these movements, LUIGI would walk with less stability. This movement is an obvious loss of energy but due to stability being of greater importance, it was ignored. The twisting is anticipated to be from the knee strike events of the outer legs. The outer legs also seemed to clash with a greater force than that of the inner legs, but the thigh pieces of the inner legs were bolted together which restricted any rotational movement.

A reoccurring problem was also the thigh shanks popping out from the knee joint. It was difficult to get a friction fit as intended, and tape was added to the thigh shank to resolve the issue. The additional tape was on a piece by piece basis, which is assumed to be due to the lack of resolution with 3D printing. Knee joints were also the point of failure due to fracturing of the plastic. Being that 3D printers print in layers, the orientation of the printed piece was always placed to have the laminations parallel to the force. The knee joint was the only section where metal inserted into the plastic. It was also the one joint that was not reamed for press fits.

For human interference, there is always the fact of inappropriate initial conditions. Although this was mitigated by launching the walker from a static position, the release angles cannot be verified as being as consistent.

6.2 Recommendations

Since it is hypothesized that the knee lock is the reason for the thigh rotation, I think it would be more reasonable to focus on the foot bracket. I would either drill a hole for a dowel rod to connect the foot bracket and shin together or 3D print the lower shin as one piece. Another recommendation would be to shrink leg lengths and increase the robustness of the walker to produce a smaller walker, which might be able to better handle added masses. In addition, building of a launch mechanism is highly recommended to cut out human error.

List of References

- [1] Peter G. Adamczyk, Steven H. Collins, and Arthur D. Kuo. The advantages of a rolling foot in human walking. *The Journal of E*, 209:3953–3956, 2006.
- [2] M. Anderson, O.C. Jenkins, and S. Osentoski. Recasting robotics challenges as experiments [competitions]. *Robotics Automation Magazine, IEEE*, 18(2):10–11, June 2011.
- [3] Barry Berman. 3-d printing: The new industrial revolution. *Business Horizons*, 55:155–162, 2012.
- [4] Vanessa F. Hsu Chen. Passive dynamic walking with knees: A point foot model. Master’s thesis, Massachusetts Institute of Technology, 2005.
- [5] Julia T. Choi, Eileen P. G. Vining, Darcy S. Reisman, and Amy J. Bastian. Walking flexibility after hemispherectomy: split-belt treadmill adaptation and feedback control. *Brain*, 132(3):722–733, 2009.
- [6] T. Chyou, G.F. Liddell, and M.G. Paulin. An upper-body can improve the stability and efficiency of passive dynamic walking. *Journal of Theoretical Biology*, 285(1):126 – 135, 2011.
- [7] Michael J. Coleman and Andy Ruina. An uncontrolled walking toy that cannot stand still. *Phys. Rev. Lett.*, 80:3658–3661, Apr 1998.
- [8] Steven H. Collins, Martijn Wisse, and Andy Ruina. A three-dimensional passive-dynamic walking robot with two legs and knees. *The International Journal of Robotics Research*, 20(7):607–615, 2001.
- [9] Laura Dyrda. 5 key trends in 3d printing medical device market, March 2015.

- [10] Mariano Garcia, Anindya Chatterjee, Andy Ruina, and Michael Coleman. The simplest walking model: Stability, complexity, and scaling. *Journal of Biomechanical Engineering*, 120:281–288, April 1998.
- [11] Mariano Sylvio Garcia. *Stability, Scaling, and Chaos in Passive-Dynamic Gait Models*. PhD thesis, Cornell University, 1999.
- [12] Lyndsey Gilpin. How biobots 5k 3d bioprinter could make doctors and medicines more effective, March 2015.
- [13] Jason Griffey. *3-D Printers for Libraries*, chapter 3: Types of Plastics, pages 13–15. ALA TechSource, July 2014.
- [14] Ismet Handžić. *Analysis and Application of Passive Gait Rehabilitation Methods*. PhD thesis, University of South Florida, 2014.
- [15] I. Handzic and K.B. Reed. Comparison of the passive dynamics of walking on ground, tied-belt and split-belt treadmills, and via the gait enhancing mobile shoe (gems). In *Rehabilitation Robotics (ICORR), 2013 IEEE International Conference on*, pages 1–6, June 2013.
- [16] I. Handzic and K.B. Reed. Validation of a passive dynamic walker model for human gait analysis. In *Engineering in Medicine and Biology Society (EMBC), 2013 35th Annual International Conference of the IEEE*, pages 6945–6948, July 2013.
- [17] I. Handzic and K.B. Reed. Perception of gait patterns that deviate from normal and symmetric biped locomotion. *Frontiers in Psychology*, 6, 2015.
- [18] A. H. Hansen, D. S. Childress, and E. H. Knox. Prosthetic foot roll-over shapes with implications for alignment of transtibial prostheses. *Prosthetics and Orthotics International*, 24(3):205–215, 2000.
- [19] C. Honeycutt, J. Sushko, and K.B. Reed. Asymmetric passive dynamic walker. In *Rehabilitation Robotics (ICORR), 2011 IEEE International Conference on*, pages 1–6, June 2011.
- [20] Craig Honeycutt. Utilizing a computational model for the design of a passive dynamic walker. Master’s thesis, University of South Florida, 2011.

- [21] Y. Ikemata, A. Sano, and H. Fujimoto. A physical principle of gait generation and its stabilization derived from mechanism of fixed point. In *Robotics and Automation, 2006. ICRA 2006. Proceedings 2006 IEEE International Conference on*, pages 836–841, May 2006.
- [22] Scott Jenkins. 3-d printing accelerates, creating cpi opportunities, February 2015.
- [23] Peter Johnston. 3-d printing: The future comes round again. *The Seybold Report*, 11, October 2011.
- [24] Derek Koop. Passive dynamic bipedal walking: Ramp - treadmill comparison and gait variation due to parameter change. Master’s thesis, University of Manitoba, 2011.
- [25] Derek Koop and Christine Q. Wu. Passive dynamic biped walking - part i: Development and validation of an advanced model. *Journal of Computational and Nonlinear Dynamics*, 2013.
- [26] Sandia National Laboratories. Getting bot responders into shape, December 2014.
- [27] Rodolfo Margaria. *Biomechanics and energetics of muscular exercise*. Clarendon Press, 1976.
- [28] TJ McCue. 3d printed prosthetics, August 2014.
- [29] T. McGeer. Passive walking with knees. In *Robotics and Automation, 1990. Proceedings., 1990 IEEE International Conference on*, pages 1640–1645 vol.3, May 1990.
- [30] Tad McGeer. Powered flight, child’s play, silly wheels and walking machines. In *Robotics and Automation, 1989. Proceedings., 1989 IEEE International Conference on*, pages 1592–1597. IEEE, 1989.
- [31] Tad McGeer. Passive Bipedal Running. *Proceedings of The Royal Society of London. Series B, Biological Sciences (1934-1990)*, 240:107–134, 1990.
- [32] Tad McGeer. Passive dynamic walking. *Int. J. of Robotics Research*, 9(2):62–82, 1990.
- [33] Simon Mochon and Thomas A. McMahon. Ballistic walking. *Journal of biomechanics*, 13(1):49–57, 1980.

- [34] M. Raibert. Dynamic legged robots for rough terrain. In *Humanoid Robots (Humanoids), 2010 10th IEEE-RAS International Conference on*, pages 1–1, Dec 2010.
- [35] H.J. Ralston. Energy-speed relation and optimal speed during level walking. *Internationale Zeitschrift fur Angewandte Physiologie Einschliesslich Arbeitsphysiologie*, 17(4):277–283, 1958.
- [36] Darcy S. Reisman, Robert Wityk, Kenneth Silver, and Amy J. Bastian. Locomotor adaptation on a split-belt treadmill can improve walking symmetry post-stroke. *Brain*, 130(7):1861–1872, April 2007.
- [37] DS Reisman, R Wityk, and AJ Bastian. Split-belt treadmill adaptation transfers to overground walking in persons poststroke. *Neurorehabil Neural Repair*, 23(7):735–744, September 2009.
- [38] J.S. Rietman, K. Postema, and J.H.B. Geertzen. Gait analysis in prosthetics: opinions, ideas and conclusions. *Prosthetics and Orthotics International*, 26:50–57, 2002.
- [39] Kazi Rushdi, Derek Koop, and Christine Q. Wu. Experimental studies on passive dynamic bipedal walking. *Robotics and Autonomous Systems*, 62(4):446 – 455, 2014.
- [40] Y. Sakagami, R. Watanabe, C. Aoyama, S. Matsunaga, N. Higaki, and K. Fujimura. The intelligent asimo: System overview and integration. pages 2478–2483, 2002.
- [41] J. Sushko, C. Honeycutt, and K.B. Reed. Prosthesis design based on an asymmetric passive dynamic walker. In *Biomedical Robotics and Biomechatronics (BioRob), 2012 4th IEEE RAS EMBS International Conference on*, pages 1116–1121, June 2012.
- [42] John Sushko. Asymmetric passive dynamic walker used to examine gait rehabilitation methods. Master’s thesis, University of South Florida, 2011.
- [43] R. Tedrake, T.W. Zhang, Ming fai Fong, and H.S. Seung. Actuating a simple 3d passive dynamic walker. In *Robotics and Automation, 2004. Proceedings. ICRA ’04. 2004 IEEE International Conference on*, volume 5, pages 4656–4661 Vol.5, April 2004.
- [44] Kalin Trifonov and Shuji Hashimoto. *Cutting Edge Robotics*, chapter 9: Active Knee-release Mechanism for Passive-dynamic Walking Machines, pages 145–153. InTech, 2010.

- [45] Wilhelm Weber and Eduard Weber. Ueber die mechanik der menschlichen gehwerkzeuge, nebst der beschreibung eines versuchs über das herausfallen des schenkelkopfs aus der pfanne im luftverdunnten raume. *Annalen der Physik*, 116(1):1–13, 1837.
- [46] Tammy White. Making sailors 'saffir' - navy unveils firefighting robot prototype at naval tech expo. Online, February 2015.
- [47] Martjin Wisse and Richard Q. van der Linde. *Delft Pneumatic Bipeds*. Springer-Verlag Berlin Heidelberg, 2007.
- [48] Q. Wu and N. Sabet. An experimental study of passive dynamic walking. *Robotica*, 22:251–262, 6 2004.
- [49] Andrew Zaleski. Ge's bestselling jet engine makes 3-d printing a core component, March 2015.

Appendices

Appendix A: 3D Printing

	CHI MEI CORPORATION																
59-1 SAN CHIA, JEN TE, TAINAN COUNTY, TAIWAN																	
TEL: 886-6-266-5000, FAX: 886-6-266-5555~7 2/2(A-GHE)																	
<u>8. EXPOSURE CONTROLS / PERSONAL PROTECTION</u>																	
<table><tr><td>Threshold Limit Value</td><td>Not determined</td></tr><tr><td>Ventilation</td><td>Necessary to exclude dust, fumes and gases.</td></tr><tr><td>Personal Protection</td><td>Eye Wear safety glasses for general purpose. Wear chemical goggles for cleaning molding machines.</td></tr><tr><td>Respiratory</td><td>Wear masks for cleaning molding machines.</td></tr><tr><td>Gloves</td><td>Necessary for handling melted resin.</td></tr></table>		Threshold Limit Value	Not determined	Ventilation	Necessary to exclude dust, fumes and gases.	Personal Protection	Eye Wear safety glasses for general purpose. Wear chemical goggles for cleaning molding machines.	Respiratory	Wear masks for cleaning molding machines.	Gloves	Necessary for handling melted resin.						
Threshold Limit Value	Not determined																
Ventilation	Necessary to exclude dust, fumes and gases.																
Personal Protection	Eye Wear safety glasses for general purpose. Wear chemical goggles for cleaning molding machines.																
Respiratory	Wear masks for cleaning molding machines.																
Gloves	Necessary for handling melted resin.																
<u>9. PHYSICAL AND CHEMICAL PROPERTIES</u>																	
<table><tr><td>Appearance</td><td>Off white pellets</td></tr><tr><td>Melting Temperature</td><td>Softening above 100°C</td></tr><tr><td>Solubility</td><td>Insoluble in water</td></tr><tr><td>Specific Gravity</td><td>1.03 ~ 1.10</td></tr></table>		Appearance	Off white pellets	Melting Temperature	Softening above 100°C	Solubility	Insoluble in water	Specific Gravity	1.03 ~ 1.10								
Appearance	Off white pellets																
Melting Temperature	Softening above 100°C																
Solubility	Insoluble in water																
Specific Gravity	1.03 ~ 1.10																
<u>10. STABILITY AND REACTIVITY</u>																	
<table><tr><td>Flammability</td><td>Yes</td></tr><tr><td>Flash Point</td><td>404 °C</td></tr><tr><td>Auto-ignition Temperature</td><td>466 °C</td></tr><tr><td>Reactivity with Water</td><td>No</td></tr><tr><td>Stability</td><td>Stable and non-reactive under normal handling and storage condition.</td></tr><tr><td>Dust Explosion</td><td>Possible if powder exists. Explosion data for powder (< 145 mesh) Lower explosion limit 45 g/m³ Minimum ignition energy 3.6 mJ Maximum explosion pressure 7 x 10⁵ Pa Maximum pressure increase rate 3.2 x 10⁷ Pa/S</td></tr><tr><td>Thermal Decomposition Gases</td><td>CO, HCN, AN, SM and NO</td></tr><tr><td>Combustion Energy</td><td>3.53 x 10⁷ J/kg (8424 Kcal/kg)</td></tr></table>		Flammability	Yes	Flash Point	404 °C	Auto-ignition Temperature	466 °C	Reactivity with Water	No	Stability	Stable and non-reactive under normal handling and storage condition.	Dust Explosion	Possible if powder exists. Explosion data for powder (< 145 mesh) Lower explosion limit 45 g/m³ Minimum ignition energy 3.6 mJ Maximum explosion pressure 7 x 10⁵ Pa Maximum pressure increase rate 3.2 x 10⁷ Pa/S	Thermal Decomposition Gases	CO, HCN, AN, SM and NO	Combustion Energy	3.53 x 10⁷ J/kg (8424 Kcal/kg)
Flammability	Yes																
Flash Point	404 °C																
Auto-ignition Temperature	466 °C																
Reactivity with Water	No																
Stability	Stable and non-reactive under normal handling and storage condition.																
Dust Explosion	Possible if powder exists. Explosion data for powder (< 145 mesh) Lower explosion limit 45 g/m³ Minimum ignition energy 3.6 mJ Maximum explosion pressure 7 x 10⁵ Pa Maximum pressure increase rate 3.2 x 10⁷ Pa/S																
Thermal Decomposition Gases	CO, HCN, AN, SM and NO																
Combustion Energy	3.53 x 10⁷ J/kg (8424 Kcal/kg)																
<u>11. TOXICOLOGICAL INFORMATION</u>																	
<table><tr><td>Irritation</td><td>Fumes or vapors generated from decomposing resin may be irritant to eyes.</td></tr><tr><td>Acute oral toxicity (LD50)</td><td>Not determined</td></tr><tr><td>Mutagenicity</td><td>Not determined</td></tr></table>		Irritation	Fumes or vapors generated from decomposing resin may be irritant to eyes.	Acute oral toxicity (LD50)	Not determined	Mutagenicity	Not determined										
Irritation	Fumes or vapors generated from decomposing resin may be irritant to eyes.																
Acute oral toxicity (LD50)	Not determined																
Mutagenicity	Not determined																
<u>12. ECOLOGICAL INFORMATION</u>																	
To avoid being taken by ocean species or birds, disposal of the waste to the ocean and water sources is inhibited.																	
<u>13. DISPOSAL CONSIDERATIONS</u>																	
Controlled incineration or landfill according to local, state or national laws and regulations concerning health and pollution. Inadequate incineration may generate toxic gases such as CO, HCN, AN and SM.																	
<u>14. TRANSPORT INFORMATION</u>																	
Not classified																	
<u>15. REGULATORY INFORMATION</u>																	
Not available																	
<u>16. OTHER INFORMATION</u>																	
None																	

Figure A.1: ABS material data sheet



Product name: NatureWorks® Polylactide Resin
Product code: 4043D Revision Number: 12 Revision date: 07/19/2006 Print date: 01/16/2009

9. PHYSICAL AND CHEMICAL PROPERTIES:

Vapor density: Not determined
Evaporation rate: No data available
Density: 1.24 g/cc
Decomposition temperature: 482F (250C)
Autoignition temperature: 388°C
Melting point/range: Not determined
Water solubility: Insoluble
Solubility in other solvents: None known

10. STABILITY AND REACTIVITY

Stability: Stable under recommended storage conditions
Conditions to avoid: Temperatures above 446F (230 °C).
Materials to avoid: Oxidizing agents. Strong bases.
Hazardous decomposition products: Burning produces obnoxious and toxic fumes. Aldehydes. Carbon monoxide (CO). carbon dioxide (CO2).
Polymerization: Not applicable

11. TOXICOLOGICAL INFORMATION

Principle Routes of Exposure: Eye contact. Skin contact. Inhalation. Ingestion.
Acute toxicity: There were no target organ effects noted following ingestion or dermal exposure in animal studies.
Local effects: May cause eye/skin irritation. Product dust may be irritating to eyes, skin and respiratory system. Caused mild to moderate conjunctival irritation in eye irritation studies using rabbits. Caused very mild redness in dermal irritation studies using rabbits (slightly irritating). Ingestion may cause gastrointestinal irritation, nausea, vomiting and diarrhoea.
Long term toxicity: Did not cause skin allergic reactions in skin sensitization studies using guinea pigs.

The Information Herein Is Given In Good Faith, But No Warranty, Express Or Implied, Is Made.
Consult the Company for Further Information.

NOTICE REGARDING MEDICAL APPLICATION RESTRICTIONS: The company does not recommend any of its products, including samples, for use: (A) in any application which is intended for any internal contact with human body fluids or body tissues (B) as a critical component in any medical device that supports or sustains human life; and (C) specifically pregnant women or in any applications designed specifically to promote or interfere with human reproduction.

Page 6 of 10

Figure A.2: PLA material data sheet

3D PRINTER

MakerBot – Replicator 2X

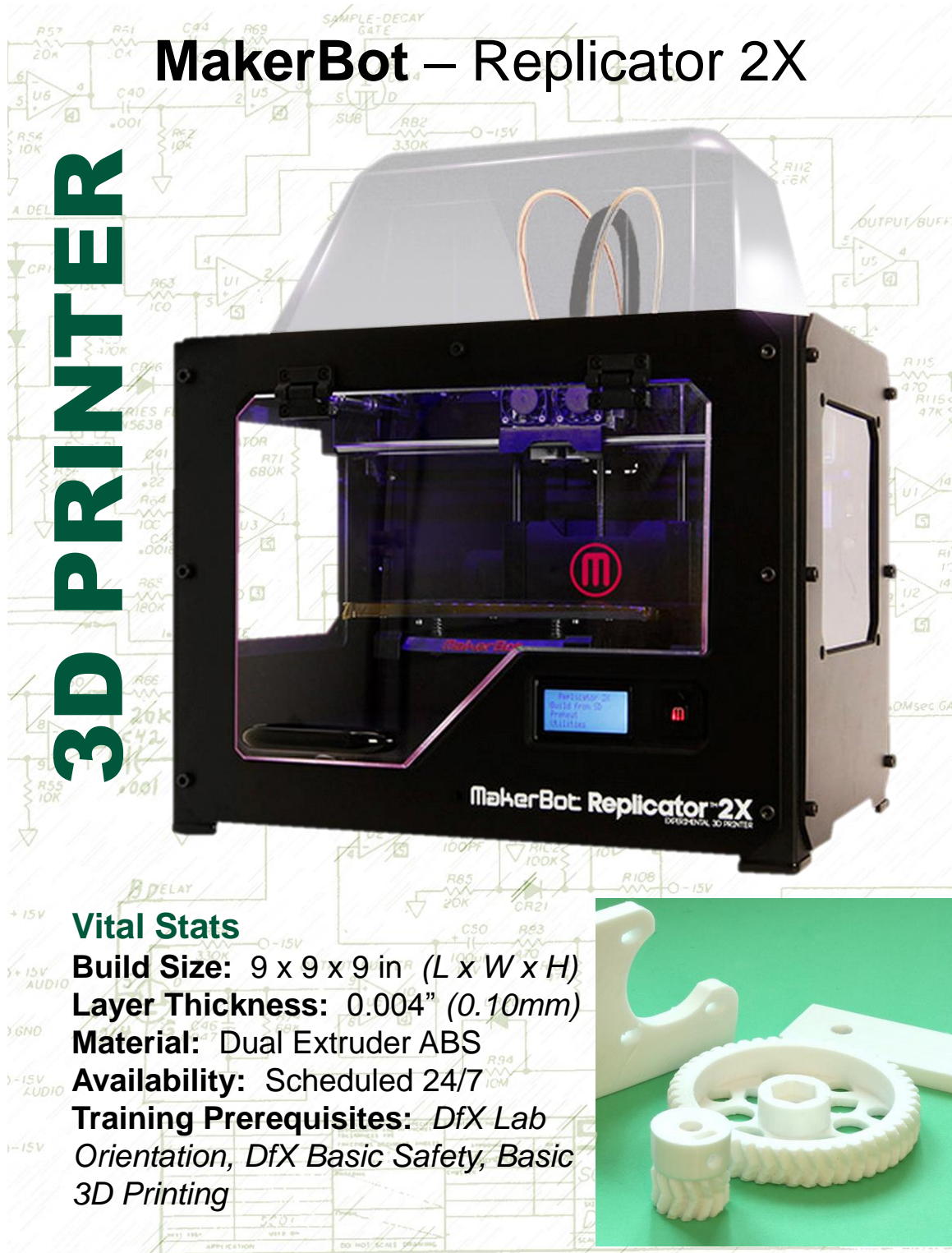
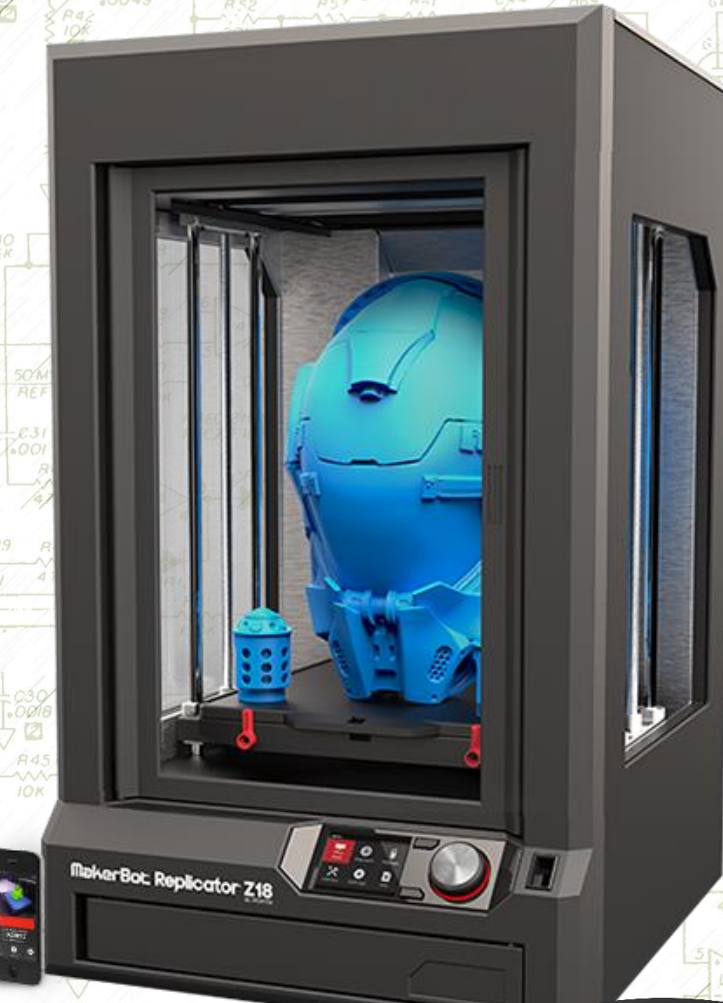


Figure A.3: MakerBot Replicator 2X

3D PRINTER

MakerBot – Replicator Z18



Vital Stats

Build Size: 12 x 12 x 18 in

Layer Thickness: 0.004" (0.10mm)

Material: Unsupported PLA

Availability: Scheduled 24/7

Training Prerequisites: DfX Lab

*Orientation, Basic 3D Printing,
Intermediate 3D Printing*



Figure A.4: MakerBot Replicator Z18

Appendix B: Damping

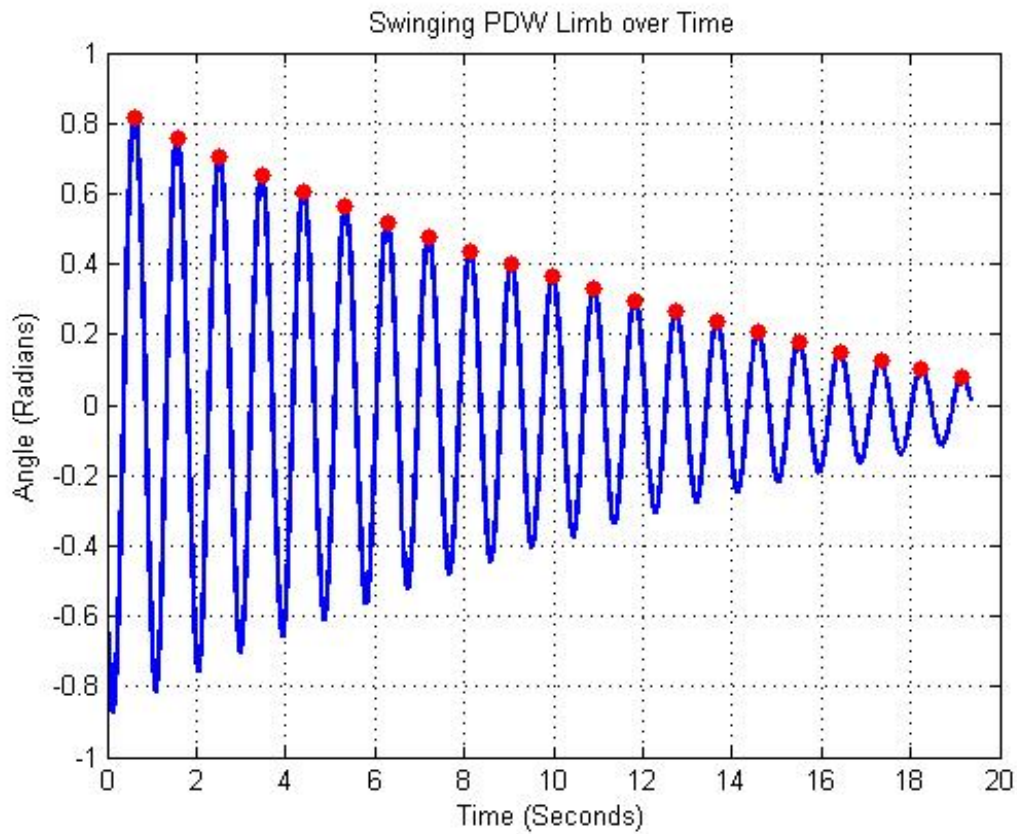


Figure B.1: Single hip bearing damping graph

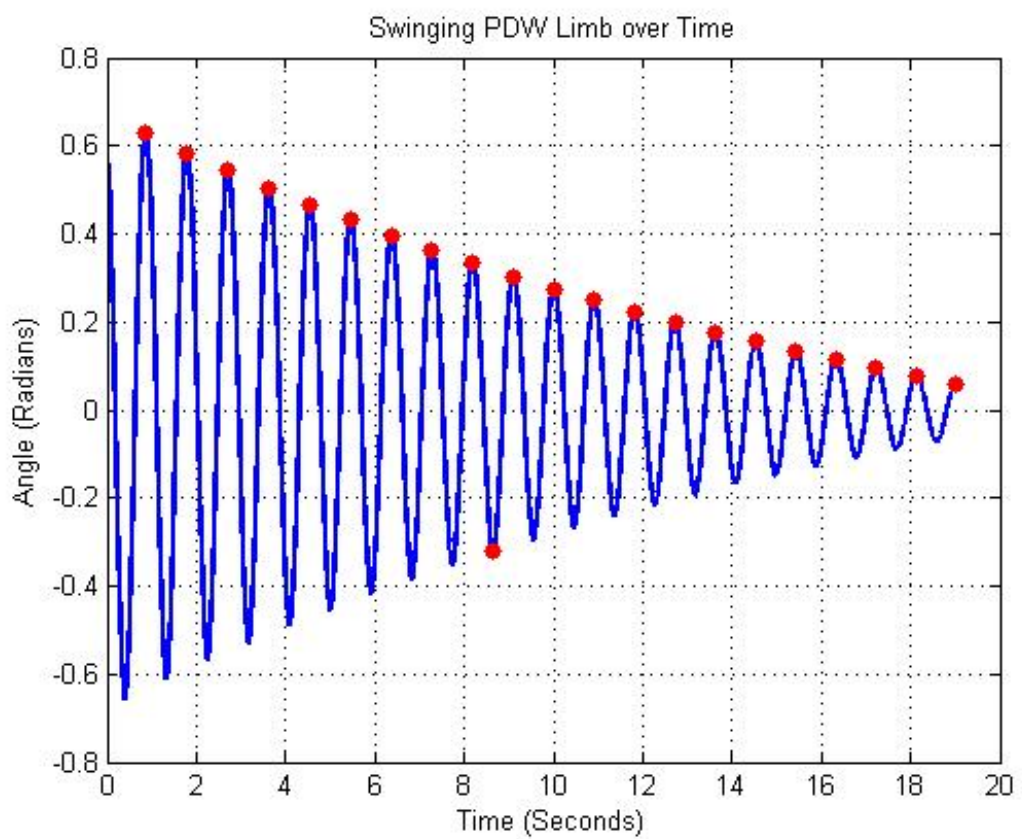


Figure B.2: Double hip bearing damping graph

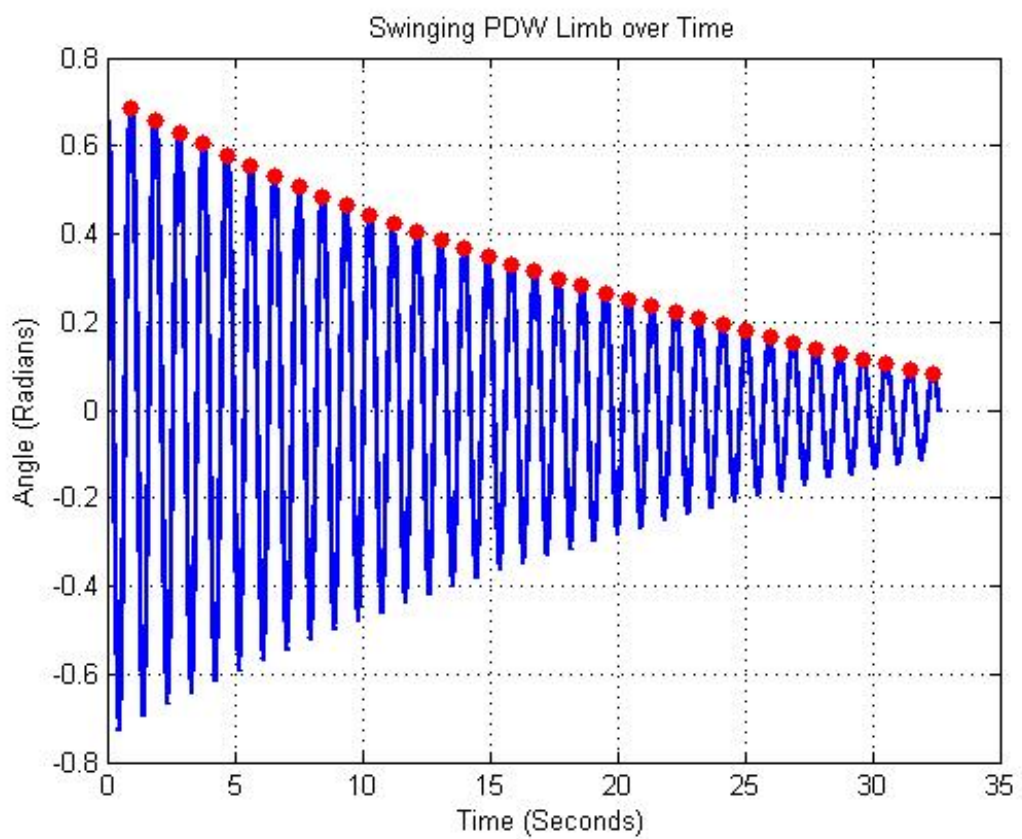


Figure B.3: Single hip bearing with lubricant

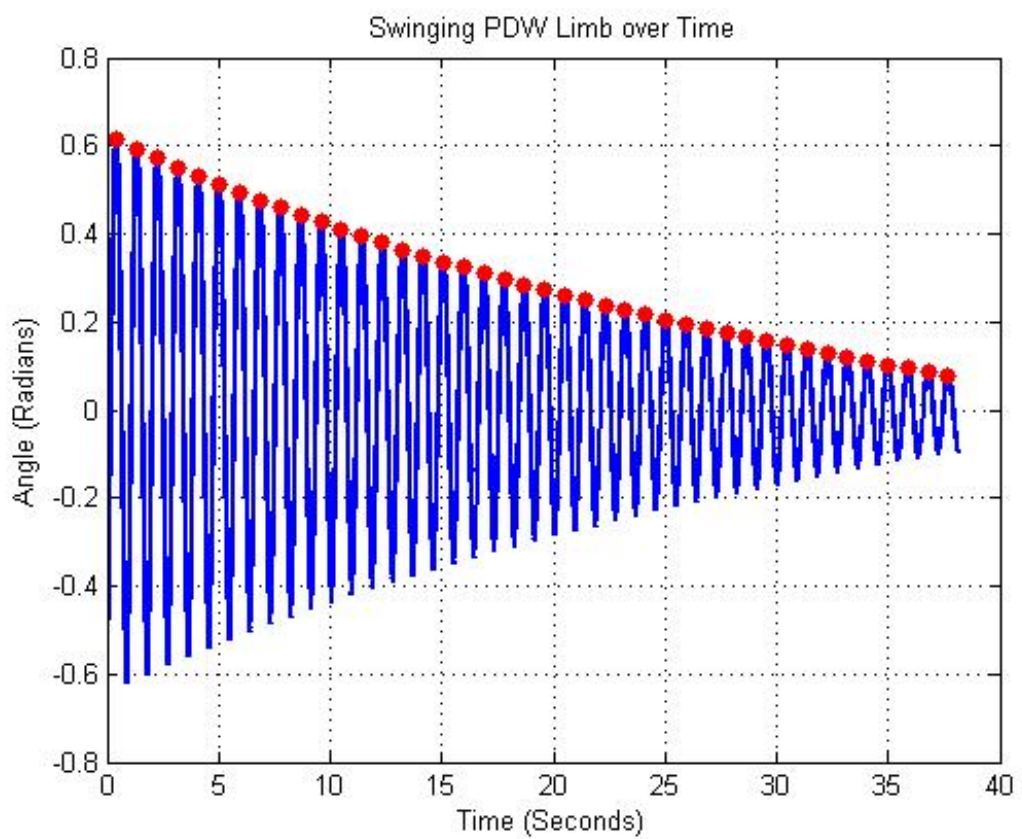


Figure B.4: Double hip bearings with lubricant

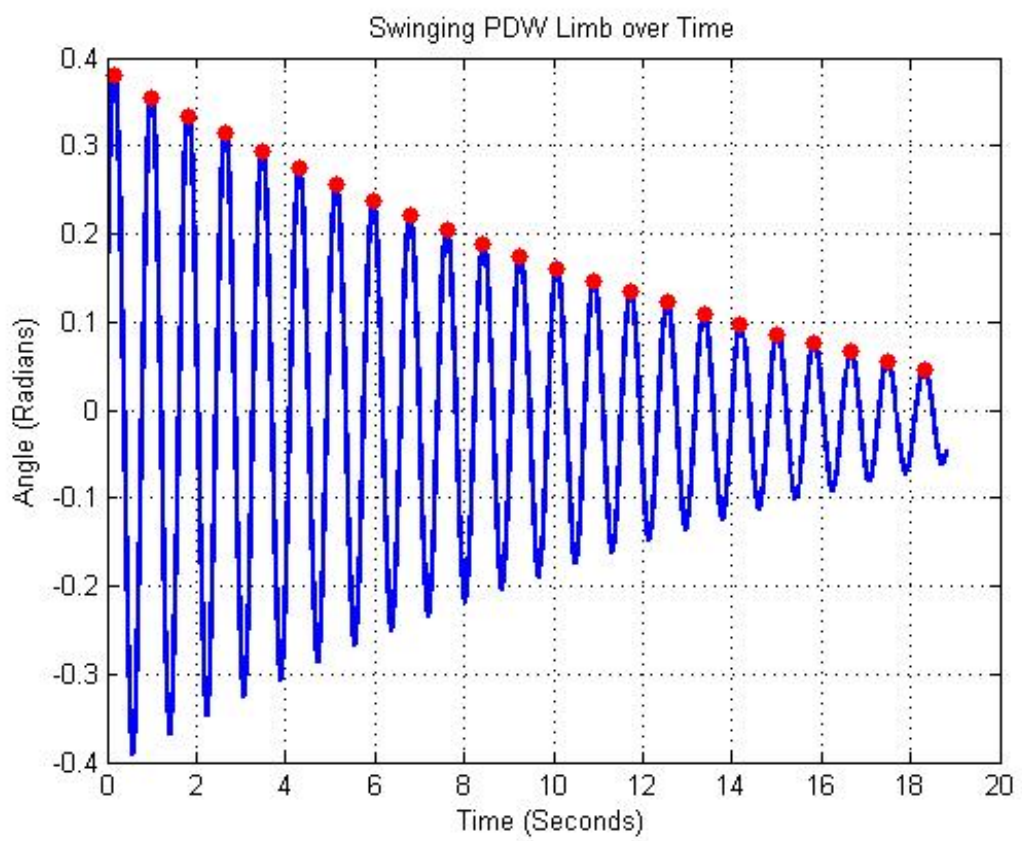


Figure B.5: Steel knee bearing

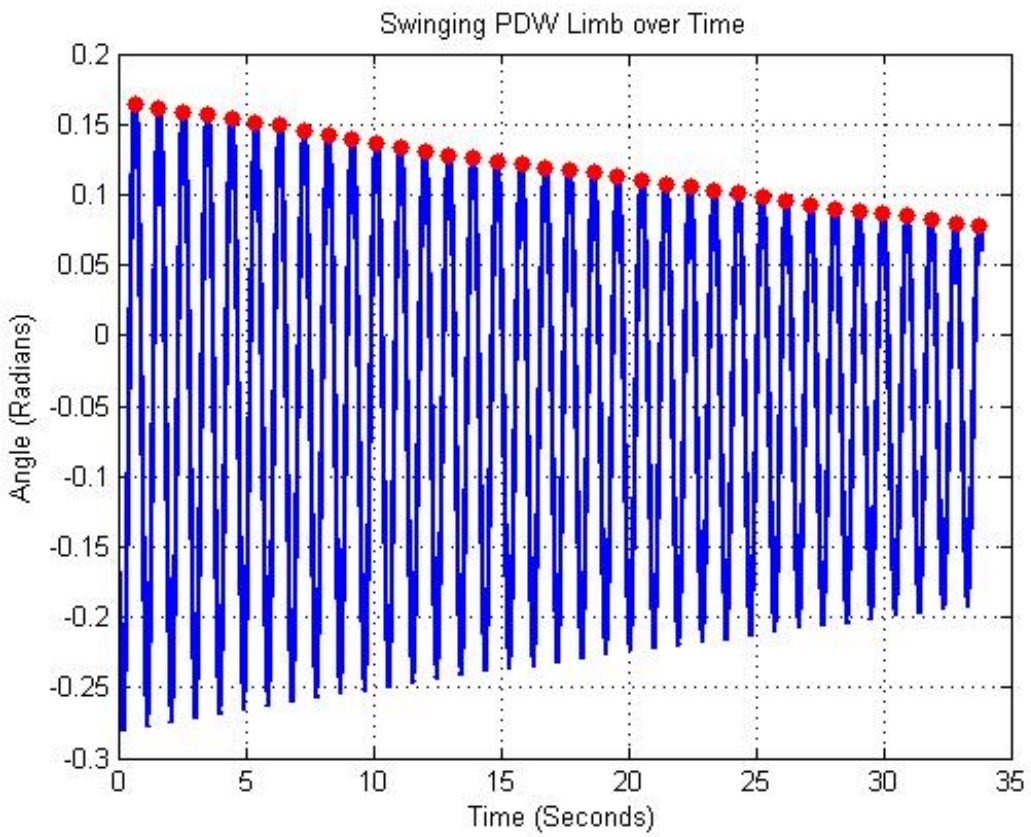


Figure B.6: Acetal knee bearing

Appendix C: Beginning of the Build

Since the author did not create the design of LUIGI a few sections of the lower body were first constructed using aluminum to gain a better understanding of the build. Knee components, hip caps, and the foot bracket were the first components to be printed. The feet were cut out of an acetate sheet and then bolted to the foot. Although it was known that the weight was too much mainly due to the bolts a general understanding of the walker and damping was gained. The LAL rod was machined out of aluminum and the LAL bolts were not yet modified to a smaller diameter.



Figure C.1: LUIGI first assembly

Appendix D: Trial Figures

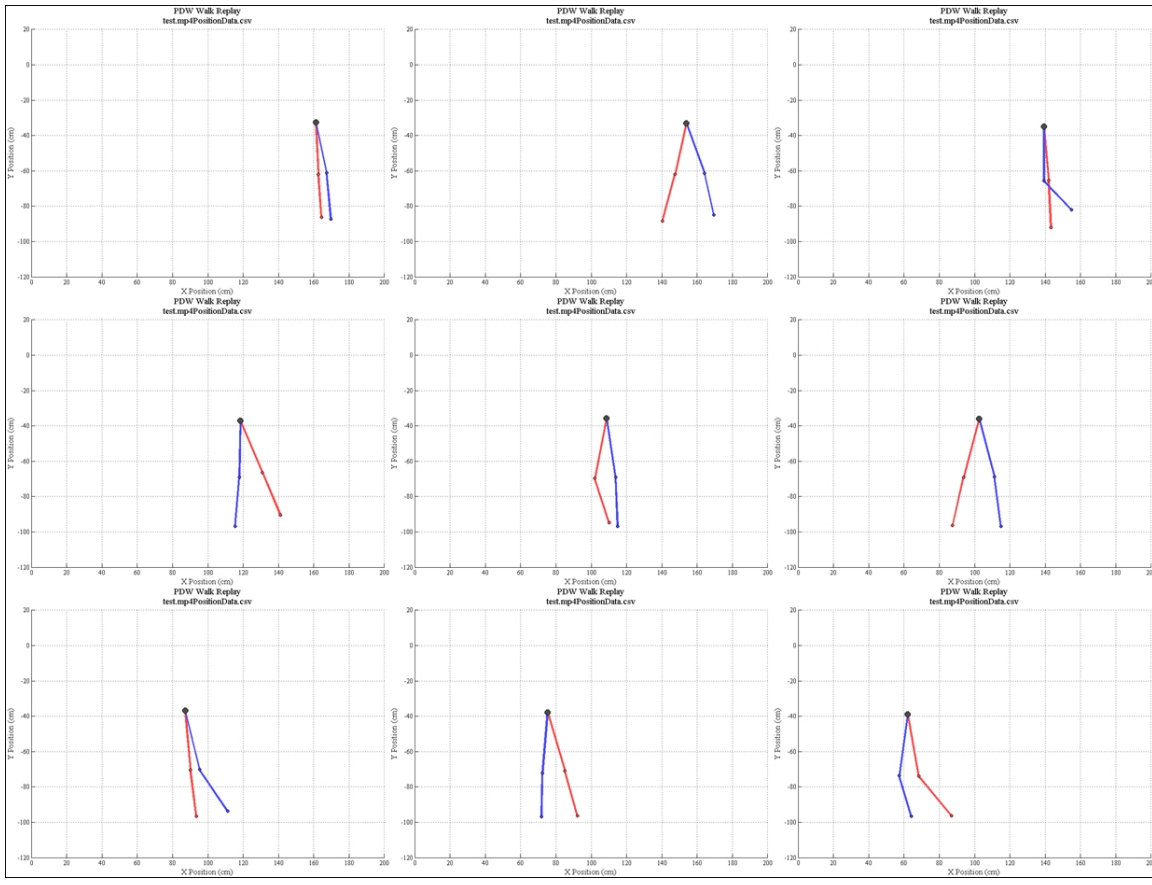


Figure D.1: Trial 1

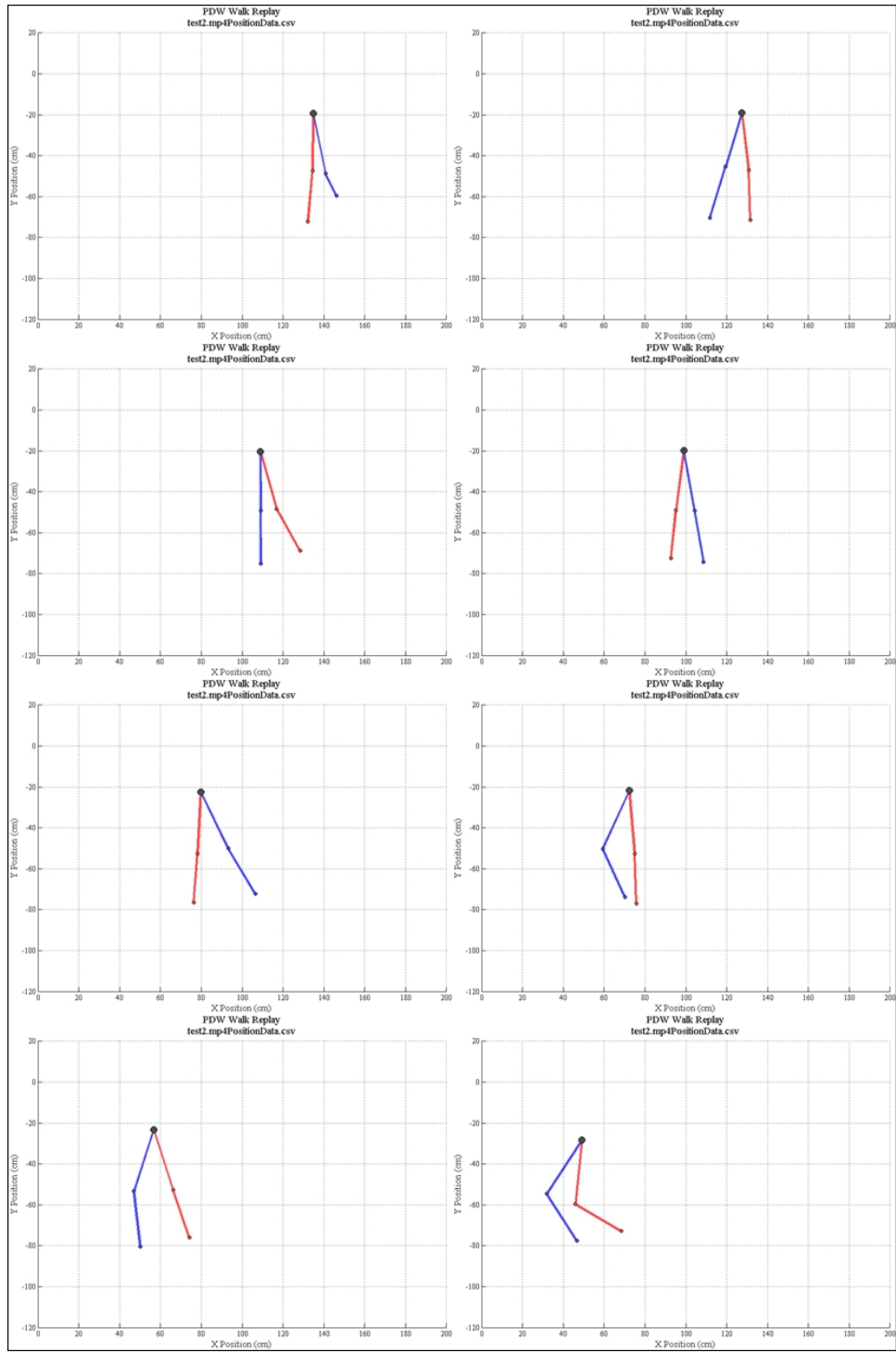


Figure D.2: Trial 2

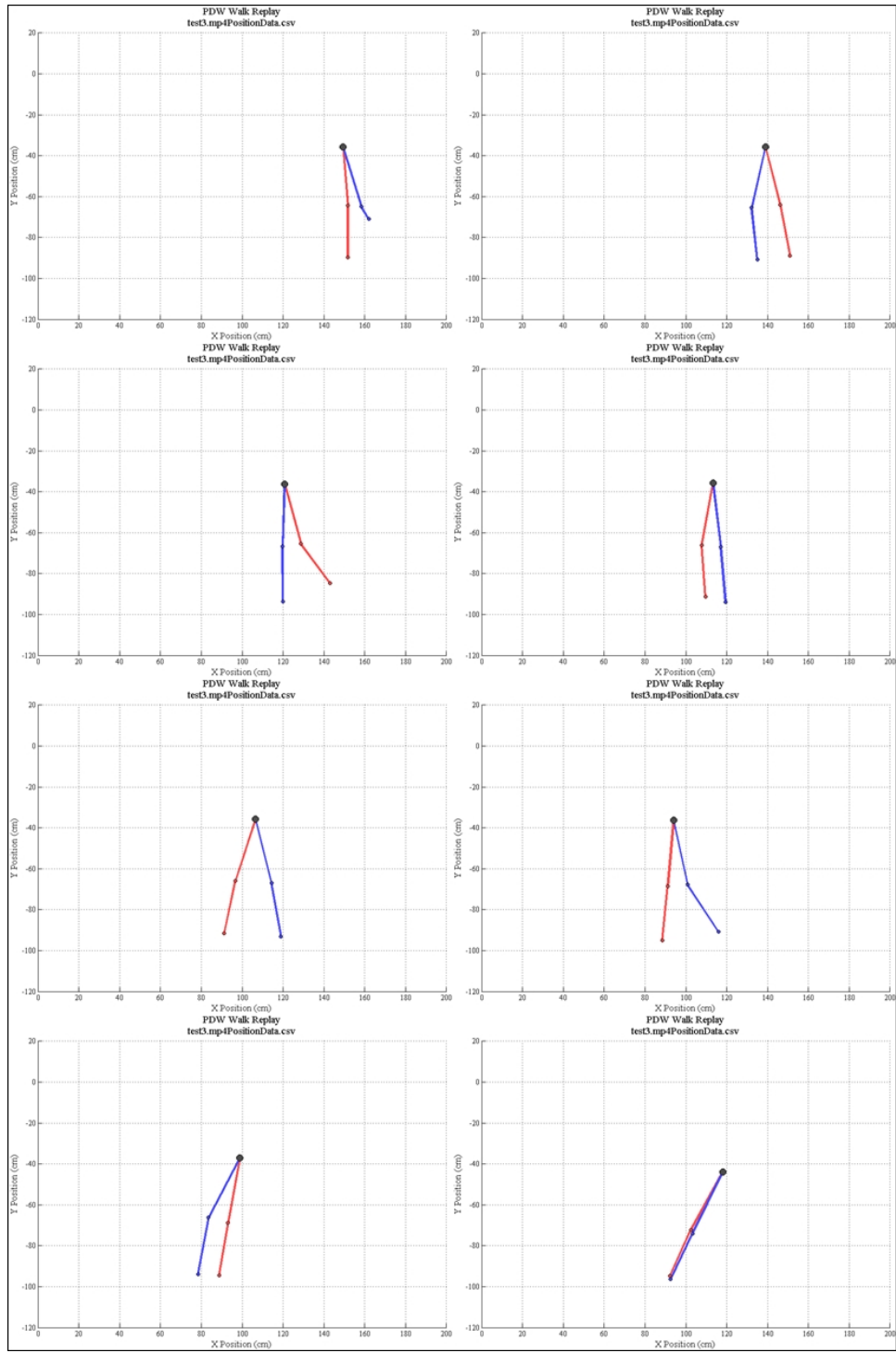


Figure D.3: Trial 3

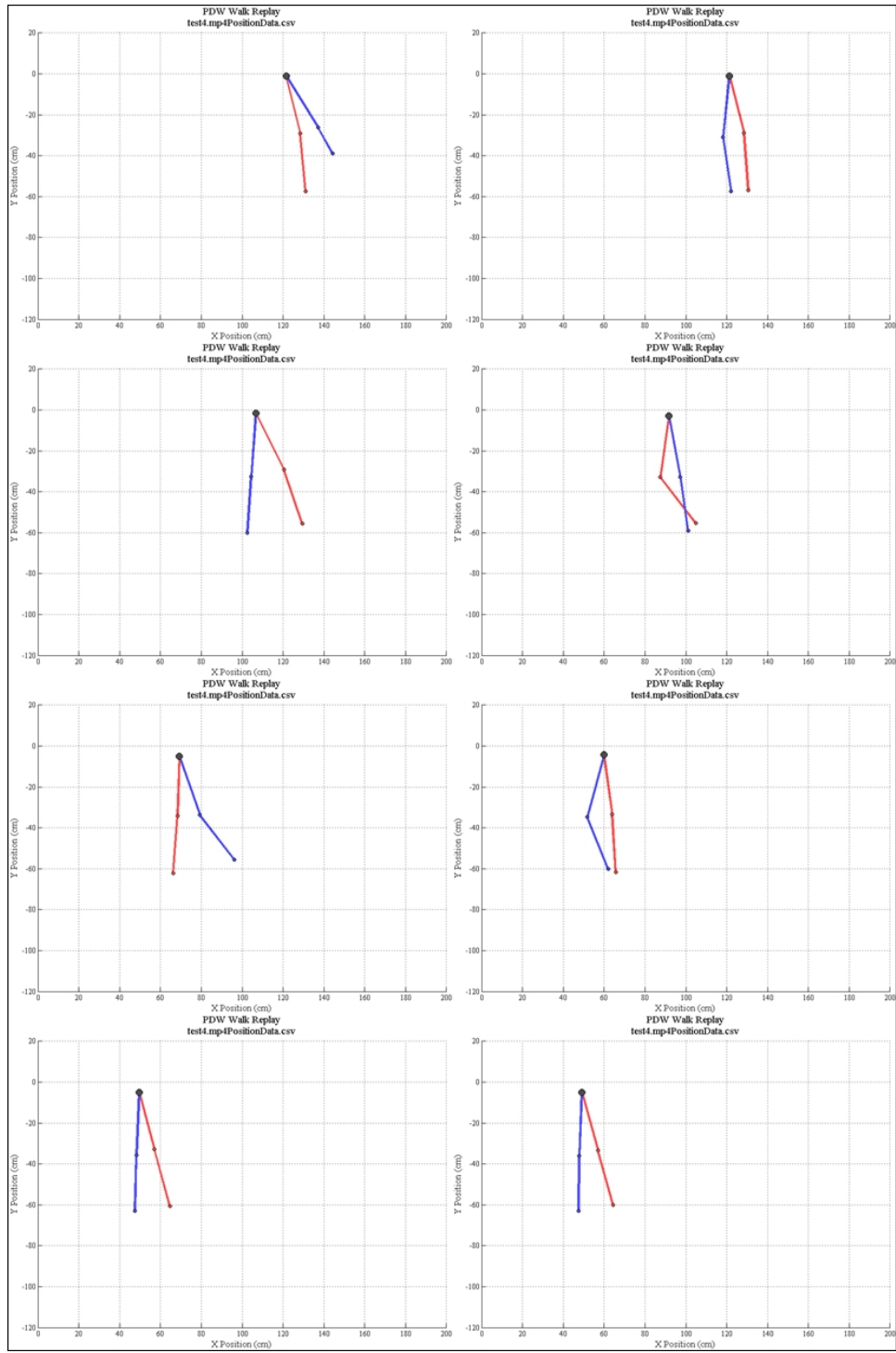


Figure D.4: Trial 4